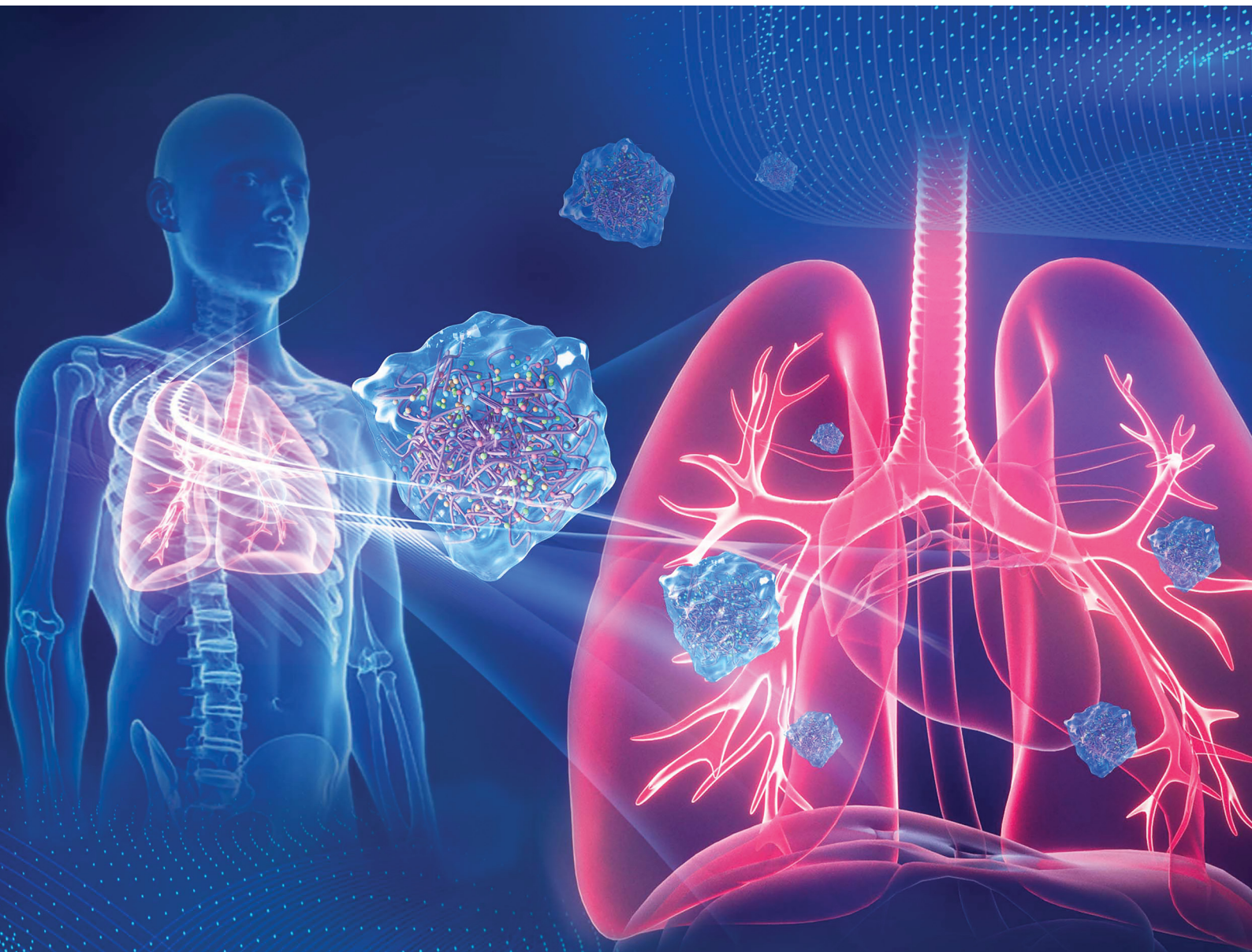


# Materials Advances

[rsc.li/materials-advances](https://rsc.li/materials-advances)



ISSN 2633-5409



Cite this: *Mater. Adv.*, 2023, 4, 5431

## Research progress on gel-based nanocomposites for diagnosis and treatment of respiratory diseases

Jing Ye,<sup>†,ab</sup> Wenjing Pei,<sup>†,ab</sup> Jing Zhu,<sup>†,c</sup> Ping Li,<sup>ab</sup> Hui Liu,<sup>ab</sup> Lei Gao,<sup>ab</sup> Changxiu Ma,<sup>ab</sup> Rongrong Gu,<sup>c</sup> Sheng Ye  <sup>\*c</sup> and Dahai Zhao<sup>\*ab</sup>

The incidence and mortality rates of respiratory diseases have been steadily increasing over the years, leading to the development of diverse diagnosis and treatment methods. Gel materials exhibit intricate structures and possess unique biological properties, making them a valuable resource in medical applications. Various types of gel materials demonstrate excellent biocompatibility, permeability and antibacterial activity, rendering them extensively used in drug delivery, release systems, anti-inflammatory and anti-infective therapies, tissue regeneration promotion, and wound healing. In this comprehensive review, we provide an overview of respiratory diseases and classify gel materials accordingly. Subsequently, we focus on the current state of gel applications in diagnosing and treatment of respiratory diseases, elaborating on the mechanisms behind the utilization of gel materials. Furthermore, we identified the limitations in the existing research of gels in respiratory diseases and anticipate their future clinical application, which promises a novel strategy for the diagnosis and treatment of respiratory diseases.

Received 17th March 2023,  
Accepted 27th June 2023

DOI: 10.1039/d3ma00129f

[rsc.li/materials-advances](http://rsc.li/materials-advances)

## 1. Introduction

Compared to other systems in the human body, the respiratory system has the highest level of exposure to the external environment due to its extensive contact area. At rest, adults inhale and exhale approximately 12 000 L of gas through the respiratory tract each day. This gas exchange occurs in 300–750 million alveoli, comprising a total surface area of about 100 square meters, where oxygen is absorbed from the external environment, and carbon dioxide is eliminated from the body. During the process of breathing, the respiratory tract and lungs can potentially encounter organic or inorganic dust in the external environment, including various microorganisms, foreign protein allergens, dust particles and harmful gases. These can lead to the development of diverse respiratory diseases. In the initial stage of pulmonary infection, virus infections are most commonly observed, frequently affecting the upper

respiratory tract. Subsequently, bacterial infection can follow. Asthma is largely associated with the inhalation of allergic substances. Exposure to particulate matter can result in pneumoconiosis, particularly silicosis, coal silicosis and asbestos silicosis. The lungs are supplied by two groups of blood vessels: the arteries and veins of the pulmonary circulation that are responsible for gas exchange, and the bronchial arteries and veins, which serve as nutrient vessels for the airway and visceral pleura. The lungs are interconnected with the blood and lymphatic circulatory systems of various organs throughout the body. Consequently, bacterial emboli from sources such as skin, soft tissue furuncles and tumor emboli can reach the lung, leading to secondary lung abscess and metastatic lung cancer, respectively. Moreover, lung disease can spread from the lungs to other organs in the body, such as lung cancer and tuberculosis affecting the lungs, bones, brain, liver and other organs.

The respiratory system is an integral component of the human body, encompassing multiple functions such as gas exchange, defense mechanisms, neuroendocrine regulation and so on. Due to its direct exposure to the external environment and frequent contact, the respiratory system is susceptible to diseases. In recent years, several factors, including the aging population, high rates of smoking, air pollution, climate changes, rapid urbanization, industrialization, and notably, an increased concentration of particles of  $\leq 2.5$  micrometers in the air, have

<sup>a</sup> Department of Respiratory and Critical Care Medicine, Second Affiliated Hospital of Anhui Medical University, Hefei, Anhui, 230601, China.

E-mail: [zhaodahai@ahmu.edu.cn](mailto:zhaodahai@ahmu.edu.cn)

<sup>b</sup> Institute of Respiratory Diseases, Second Affiliated Hospital of Anhui Medical University, Hefei, Anhui, 230601, China

<sup>c</sup> College of Science & School of Plant Protection, Anhui Agricultural University, 130 Changjiang West Road, Hefei, Anhui 230036, China.

E-mail: [sye503@ahau.edu.cn](mailto:sye503@ahau.edu.cn)

† These authors contributed equally.



contributed to a steady rise in the incidence and mortality of respiratory diseases.<sup>1</sup> Since 2017, respiratory diseases have emerged as the third leading cause of disability and death globally, following cardiovascular diseases and cancer. Respiratory diseases are broadly categorized based on the anatomical structure and pathophysiological characteristics of the respiratory system. These categories include (a) airflow-restricted lung disease, (b) restrictive pulmonary disease with ventilation dysfunction, and (c) pulmonary vascular diseases. Infections and tumors represent two major factors that can impact the respiratory system, resulting in various pathological changes. Common clinical manifestations of respiratory diseases encompass cough, expectoration, chest tightness, wheezing, and chest pain. In severe cases, respiratory difficulties and respiratory failure can occur. Additionally, the global COVID-19 pandemic has heightened worldwide attention towards the diagnosis and treatment of respiratory diseases.

Clinical medicine and biomaterials are two interrelated fields that contribute to achieving precise medical objectives in the diagnosis and treatment of various diseases. Traditional medicine faces several limitations and challenges, including poor bioavailability, systemic toxicity, inadequate targeting specificity and suboptimal diagnostic and therapeutic efficacy. To address these limitations, Chen introduced the interdisciplinary field of “materdicine”.<sup>2</sup> Modern biomaterial science has led to the development of numerous products such as drug-eluting stents, artificial heart valves, and artificial hip joints, significantly benefiting human health. Biomaterials can be classified into four types based on their properties: metal materials, ceramic materials, polymer materials and composite materials. Gel, being polymer materials that contain liquid, are self-supporting and stable dispersion system, characterized by a continuous grid structure composed of single chains or large molecular aggregates.<sup>3</sup> Gel structures are complex, and gel phenomena are widespread in nature. Most organisms consist of soft gel-like substances that contain water. A diverse range of gel materials with various properties have found widespread applications in the field of medical biology, allowing for the customization and functionalization of gels. Gel-based nanocomposites refer to three-dimensional network system formed through the physical or chemical crosslinking of high molecular polymers.<sup>4</sup> Nano-gels exhibit high water absorption, structural modifiability, high drug loading capacity and good biocompatibility, making them excellent carriers for various drugs, including biomacromolecules.<sup>5,6</sup> In addition, the use of nanoparticles holds significant potential for enhancing diagnostic imaging and enabling unique treatments for lung diseases. Presently, the diagnosis of respiratory diseases relies on detailed medical histories and physical examinations, with imaging techniques such as chest X-ray and computed tomography (CT) playing a crucial role. With the advancement of precision medicine, there is an increasing demand for more sophisticated diagnostic methods to identify specific pathogens or pathologies. Moreover, the treatment of respiratory diseases extends beyond intravenous infusion and oral administration, with clinical practice increasingly incorporating drug delivery methods and

minimally invasive surgeries. Many of these rapidly evolving diagnostic and treatment approaches methods of diagnosis and treatment are closely related to various gel materials, especially in the areas of drug delivery and release, anti-inflammatory and anti-infective therapies, tissue regeneration promotion and wound healing.<sup>7-11</sup>

This review provides an overview of the classification of respiratory diseases and gels (Fig. 1), with a specific emphasis on their application in the diagnosis and treatment of respiratory diseases, including lung cancer. Furthermore, we delve into the mechanisms underlying the utilization of gel materials in the diagnosis and treatment of respiratory diseases. We expect that the application of gel as a biomaterial in the field of respiratory diseases will offer a broader prospect, thereby providing healthcare professionals with new strategies for effectively treating respiratory diseases.

## 2. Overview of respiratory diseases

### 2.1 Restrictive pulmonary disease with ventilation dysfunction

Patients with restrictive lung disease experience incomplete lung expansion, preventing the lungs from being fully filled with air. Interstitial lung disease (ILD), also known as diffuse pulmonary parenchymal disease, is the most common form of restrictive respiratory dysfunction. ILD encompasses various types, with idiopathic pulmonary fibrosis (IPF) accounting for 20% to 50% of all ILD cases.<sup>12</sup> The estimated incidence of IPF in Europe and North America ranges from 3 to 9 cases per 100 000 people per year, while it is lower in Asia and South America.<sup>13</sup> As inflammation, fibrosis, and diffusion capacity deteriorate, patients with ILD experience hypoxemia, decreased blood oxygen saturation, as well as shortness of breath and dyspnea. Chronic hypoxemia may lead to cyanosis, while increased dyspnea can result in weight loss and malnutrition.<sup>14</sup> Patients with ILD are characterized by restrictive ventilation dysfunction and gas exchange dysfunction.<sup>15</sup> High-resolution computed tomography (HRCT) plays a key role in diagnosing IPF and often eliminates the need for invasive diagnostic procedures. Usually, HRCT typically reveals usual interstitial pneumonia (UIP), which refers to the histopathological changes commonly observed in IPF patients, such as honeycombing.<sup>16</sup> Therefore, the clinical diagnosis of a certain ILD is a dynamic process that requires close collaboration among clinical, radiological and pathological experts to verify or modify the diagnosis based on comprehensive data. Different types of interstitial lung diseases require distinct treatment approaches. The primary goals of treatment are to prevent or reduce pulmonary inflammation and fibrosis, improve patients' quality of life and prolong survival. In clinical practice, there are three main treatment approaches for ILD: drug therapy, oxygen therapy and surgical interventions.<sup>17,18</sup>

Restrictive ventilation defects can also arise from musculoskeletal abnormalities in the thoracic cavity or respiratory muscle weakness caused by neuromuscular diseases. Acute idiopathic



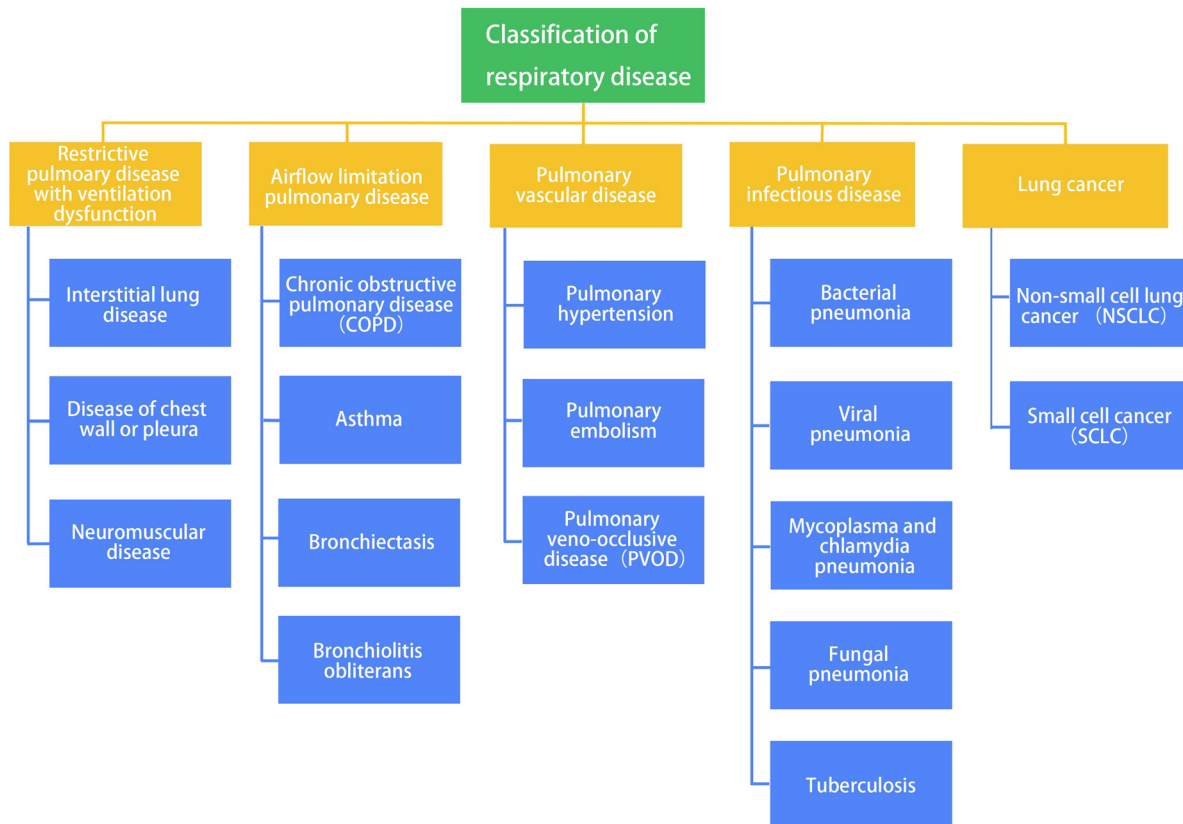


Fig. 1 Classification of respiratory diseases.

demyelinating polyneuropathy (Guillain-Barré syndrome), motor neuron disease, and poliomyelitis are recognized conditions that can result in respiratory insufficiency.<sup>19,20</sup>

Additionally, restrictive ventilation dysfunction can be caused by chest wall and pleural diseases. In stage III (dorsal or thoracic) of ankylosing spondylitis (AS), patients may experience chest and thoracoabdominal pain, along with limited thorax expansion due to inflammation-related damage to the costovertebral and sternocostal joints pleural effusion,<sup>21,22</sup> whether caused by tuberculosis, tumors, connective tissue diseases, or other pleural diseases such as pleural mesothelioma, can also restrict the expansion of thoracic or lung tissue and reduce the compliance of thoracic and/or lung.<sup>23</sup>

Furthermore, obesity can contribute to significant restrictive lung physiology and give rise to obesity hypoventilation syndrome (OHS).<sup>24</sup> Individuals with severe obesity may experience severe and potentially life-threatening respiratory complications. Restrictive hypoventilation caused by decreased chest wall compliance and diaphragm dysfunction is more pronounced in male and abdominal obese subjects.<sup>25</sup>

## 2.2 Airflow limitation pulmonary diseases

Airflow limitation pulmonary diseases encompass a group of lung diseases characterized by ventilation dysfunction. The exact pathogenesis of these diseases remains complex and not fully understood. The group includes chronic obstructive pulmonary disease (COPD), which involves persistent airflow

restriction, as well as bronchial asthma, which exhibits reversible airflow restriction, bronchiectasis and bronchiolitis obliterans. These diseases significantly impact patients' ability to perform physical labor and diminish their overall quality of life.

**2.2.1 COPD.** COPD is a prevalent, preventable, and treatable disease commonly observed in elderly patients, particularly those aged 65 and above. It is characterized by persistent respiratory symptoms and limited airflow, which is often associated with abnormalities in the airway and/or alveolar resulting from significant exposure to harmful particles or gases.<sup>26</sup> Smoking is the primary risk factor for COPD.<sup>27</sup> Other causes include air pollution, indoor biomass fuel burning, dust occupational exposure, chemical agents and dust.<sup>28–30</sup> In the examinations of lung function, a post-bronchodilator forced expiratory volume in one second (FEV1) to forced vital capacity (FVC) ratio less than 0.70 is commonly used as a diagnostic criterion for COPD. The primary goal of COPD treatment is to prevent and control symptoms, reduce the severity and frequency of acute exacerbations, improve respiratory capacity, enhance exercise tolerance and reduce mortality. Treatment approaches involve reducing exposure to risk factors, comprehensive disease assessment, patient education, both pharmacological and non-pharmacological interventions for stable COPD, and prevention and treatment of acute exacerbations of COPD.<sup>31</sup>

**2.2.2 Asthma.** Asthma is a chronic inflammatory disease of the airway characterized by intermittent airway obstruction and



heightened reactivity. Various cell types, including mast cells, eosinophils, T lymphocytes, macrophages, neutrophils and epithelial cells play a role in the pathogenesis of asthma. In susceptible individuals, inflammation leads to airway hyperresponsiveness, resulting in recurrent symptoms such as wheezing, shortness of breath, chest tightness or cough.<sup>32</sup> Diagnosis of asthma is established when patients exhibit typical symptoms and signs, along with evidence of airflow limitation, such as positive bronchodilator reversibility (BDR) or provocation test.<sup>33</sup> The treatment of asthma focuses on both acute exacerbations and long-term management. The general principles for the treatment of acute bronchial asthma are anti-inflammatory, antispasmodic, antiasthmatic, antiallergic and symptomatic treatment to alleviate symptoms promptly. The treatment of asthma in remission aims at long-term control of symptoms, anti-inflammatory measures reduction of airway hyperresponsiveness, avoidance of triggers, and self-care.<sup>34</sup> Medications commonly used for asthma treatment include glucocorticoids, mast cell membrane stabilizers, leukotriene receptor antagonists, bronchodilators, theophylline and anticholinergic drugs. In recent years, specific immunotherapy methods have also been developed as a treatment option for asthma.

**2.2.3 Bronchiectasis.** Bronchiectasis is a condition characterized by the chronic inflammatory reaction of the bronchi and surrounding lung tissues, resulting in the destruction of the bronchial wall and the formation of irreversible expansion and degeneration of the airway lumen. Clinical symptoms commonly associated with bronchiectasis include chronic cough, the production of large amounts of purulent phlegm, and recurrent hemoptysis. Pulmonary function test typically reveals obstructive ventilation dysfunction as the main manifestation.<sup>35</sup> The development of bronchiectasis is attributed to a variety of triggering factors, which contribute to a vicious circle of airway remodeling and dilation.<sup>36</sup> High-resolution chest CT is an important method to diagnose bronchiectasis. Treatment objectives focus on relieving symptoms, improving the quality of life, protecting lung function, and reducing overall morbidity and mortality rates.<sup>37</sup>

**2.2.4 Bronchiolitis obliterans.** Bronchiolitis obliterans (BO) is a rare fibrotic disease involving terminal bronchioles and respiratory bronchioles. It is characterized by clinical manifestations such as recurrent or persistent shortness of breath, wheezing or coughing, poor exercise tolerance, wet squeaking sounds in the lungs, lack of response to bronchodilators, and obstructive pulmonary dysfunction.<sup>38</sup> The most common causes of BO include lower respiratory tract infection in children,<sup>39</sup> hematopoietic stem cells or lung and heart-lung transplantation,<sup>40,41</sup> and inhalation of toxic fumes.<sup>42</sup> High-resolution CT scans are typically the first choice for evaluating suspected or confirmed BO patients. Currently, there is no standardized and effective treatment plan for BO. However, to control the progression of BO, clinical management often involves the use of glucocorticoids, immunosuppressants, immunomodulatory drugs and targeted therapies.

### 2.3 Pulmonary vascular diseases

Pulmonary vascular diseases mainly include primary and secondary pulmonary hypertension as well as pulmonary veno-occlusive disease (PVOD). Pulmonary arterial hypertension (PAH) is a progressive disorder characterized by elevated pulmonary arterial pressure (mean >25 mm Hg at rest or >30 mm Hg during exercise), normal pulmonary wedge pressure, and subsequent right heart failure.<sup>43</sup> The development of primary pulmonary hypertension (PPH) involves the interaction between genetic susceptibility and environmental factors. As PPH is a progressive disease, there is currently no curative treatment available. The main goal of treatment is to reduce pulmonary artery pressure, alleviate symptoms and improve prognosis. Pulmonary thromboembolism (PTE) is the most common secondary pulmonary hypertension. PTE arises when a thrombus originating from venous system or right heart obstructs the pulmonary artery or its branches. Deep vein thrombosis (DVT) of lower limbs is a major source of thrombi causing PTE. PTE and DVT together constitute thromboembolism (VTE), representing different clinical manifestations of VTE in distinct locations and stages.<sup>44</sup> Clinical manifestations of PTE include chest pain, dyspnea, hemoptysis and so on. However, these symptoms lack specificity, which can lead to misdiagnosis if not thoroughly evaluated.

PVOD is a clinicopathological syndrome that can cause pulmonary hypertension. It is characterized by progressive occlusion of pulmonary venules, resulting in increased pulmonary vascular resistance and right heart failure.<sup>45</sup> The incidence of PVOD ranges from approximately 0.1 to 0.2 cases per million individuals. The onset of PVOD can occur at any age, with the majority of cases occurring under 50 years old. The incidence in children is similar between boys and girls, while in adult men, it is higher.<sup>46</sup> The clinical manifestations of PVOD are nonspecific, with the most prominent symptom being the progressive worsening of dyspnea following exercise. The diagnosis of PVOD still relies on surgical lung biopsy as the gold standard. However, other diagnostic tools such as high-resolution CT scans, arterial blood gas analysis, pulmonary function and bronchoalveolar lavage fluid (BALF) can also be helpful.<sup>47</sup> Currently, the primary focus of PVOD treatment is to alleviate symptoms, restrict physical activities, and avoid medications that may worsen pulmonary hypertension, such as  $\beta$ -blockers. Traditional medical treatment options include oxygen inhalation, diuretics, cardiac medications and anticoagulation.<sup>48</sup>

### 2.4 Pulmonary infectious diseases

**2.4.1 Pneumonia.** Pneumonia can be classified into different types based on its etiology. Bacterial pneumonia is caused by various bacteria, including *Streptococcus pneumoniae*, *Staphylococcus aureus*, *Klebsiella pneumoniae*, *Pseudomonas aeruginosa* and *Escherichia coli*. Atypical pathogen pneumonia is caused by organisms such as mycoplasma, chlamydia and Legionella. Viral pneumonia is caused by viruses like adenovirus, respiratory syncytial virus, coronavirus and influenza virus. Fungal pneumonia is caused by fungi such as *Aspergillus*,



Candida and Cryptococcus. Identifying the specific pathogens responsible for pneumonia is crucial for accurate diagnosis and appropriate treatment. Traditional methods for identifying pathogens can include culture of sputum, blood, pleural effusion or BALF, as well as special staining and smear techniques. However, in recent years, Next-generation sequencing (NGS) technologies have become increasingly prevalent in clinical settings and have shown significant advantages. NGS involves extracting pathogenic DNA or RNA from sputum or BALF samples and sequencing the genetic material to identify the specific pathogen causing the infection.<sup>49</sup>

**2.4.2 Pulmonary tuberculosis.** Tuberculosis (TB) is a chronic infectious disease caused by *Mycobacterium tuberculosis* (MTB) infection. It is a significant public health issue and the leading cause of death worldwide caused by a single pathogen.<sup>50</sup> While MTB primarily infects the lungs, but it can also infect almost any organ system, including lymph nodes, central nervous system, liver, bones, genitourinary tract and gastrointestinal tract. Tuberculosis is highly transmissible through respiratory droplets. In 2021, tuberculosis resulted in 1.5 million deaths.<sup>51</sup> Traditional methods for detecting TB pathogens include acid-fast staining smear and mycobacterial culture. However, with the advancement of molecular biology techniques, molecular diagnosis, especially Xpert MTB/Rif assay, has gained more and more attention due to its high sensitivity, specificity, simplicity, and rapidity.<sup>52</sup> Chemotherapy plays a crucial role in the management of tuberculosis, serving as both a powerful treatment approach and an essential component of disease prevention and control. However, in recent years, the incidence and mortality rates of multidrug-resistant (MDR) and extensively drug-resistant (XDR) tuberculosis have been increasing. The management of MDR and XDR involves comprehensive treatment strategies centered around chemotherapy, including immunotherapy, interventional therapy, and surgical interventions.<sup>53</sup>

## 2.5 Lung cancer

Lung cancer is the most common cancer among men worldwide and the second most common cancer among women, following breast cancer. Lung cancer is also the main cause of cancer-related death for both genders.<sup>54</sup> Several factors contribute to the increasing incidence of lung cancer, including smoking, exposure to indoor and outdoor air pollution, occupational exposure to harmful substances, genetic susceptibility, radiation exposure, and an unbalanced diet.<sup>55–57</sup> Lung cancer can be classified into two main pathological types: non-small cell lung cancer (NSCLC) and small cell lung cancer (SCLC). NSCLC accounts for about 85% of and is further divided into squamous cell carcinoma (LSCC) and adenocarcinoma (LADC).<sup>58</sup> The different pathological types have distinct characteristics and require different treatment approaches. Early diagnosis and accurate determination of pathological types of lung cancer are the keys to improve the survival rate and prognosis of lung cancer patients. There are many ways to obtain pathological samples for diagnosis, such as fiberoptic bronchoscopy, thoracoscope, CT-guided percutaneous lung

puncture and so on. Serum tumor markers, such as Carcinoembryonic antigen (CEA), Cytokeratin 19 fragment (CYFRA21-1) and Neuron-specific enolase (NSE), are non-invasive tests that can aid the diagnosis of primary lung cancer.<sup>59–62</sup> The treatment approach for lung cancer should be based on factors such as the patient's physical condition, pathological type, molecular pathological diagnosis, and clinical stage. Treatment options include surgery, chemotherapy, targeted therapies, immunotherapy and radiotherapy. A comprehensive and personalized treatment plan aims to achieve complete tumor eradication or maximum tumor control, increase cure rates, improve patients' quality of life, and prolong survival time.<sup>63</sup>

## 3. Classification of gels

There are many kinds of gel materials, and their classification can be quite intricate. Based on the variations in molecular structures, gels can be divided into polymer gels, supramolecular gels and metal-organic framework gels. Each type of gels possesses distinct characteristics and finds applications in diverse fields. In this section, we provide a straightforward classification focused on the gels discussed in this review.

### 3.1 Polymer gel

A polymer gel is a three-dimensional or interpenetrating network (IPN) composed of macromolecular chains and a solvent. Based on the source of the polymer, it can be categorized as either natural polymer gel or synthetic polymer gel. The conventional method for preparing polymer gels involves the initiation, polymerization, and cross-linking of monomers using initiators and cross-linking agents. Several types of polymer gels have been synthesized using various radiation methods, such as poly (*N*-isopropylacrylamide) (pNIPAAm) hydrogel,<sup>64</sup> polyvinyl pyrrolidone (PVP),<sup>65</sup> poly(acrylic acid/acrylamide) gel,<sup>66</sup> and hydroxypropyl cellulose methacrylate (HPCM) gel,<sup>67</sup> as illustrated in Fig. 2. The radiation methods include  $\gamma$ -ray, ion and UV radiation. The incorporation of IPN technology allows for the formation of a unique topological entanglement between the blended components of the polymer network. This interweaving interaction leads to specific properties, thereby greatly improve the mechanical properties of products. PH- and electric-responsive sensitive polymer gels have been synthesized through graft copolymerization and polymer IPN technology.<sup>67,68</sup> Polymer gel have found widespread applications in memory element switches, sensors, drug-controlled release system, artificial muscles, and the encapsulation of active enzymes.

### 3.2 Supramolecular gel

Supramolecular polymer gel is a type of nanostructures formed by the assembly of small molecules into supramolecular polymers, which then undergo multi-level assembly through various noncovalent interactions to form the gel. There are several ways to classify supramolecular gels:<sup>69</sup> (1) based on the fixed solvent, they can be divided into organic gel, hydrogel and ionic liquid gel according to the fixed solvent, similar to polymer



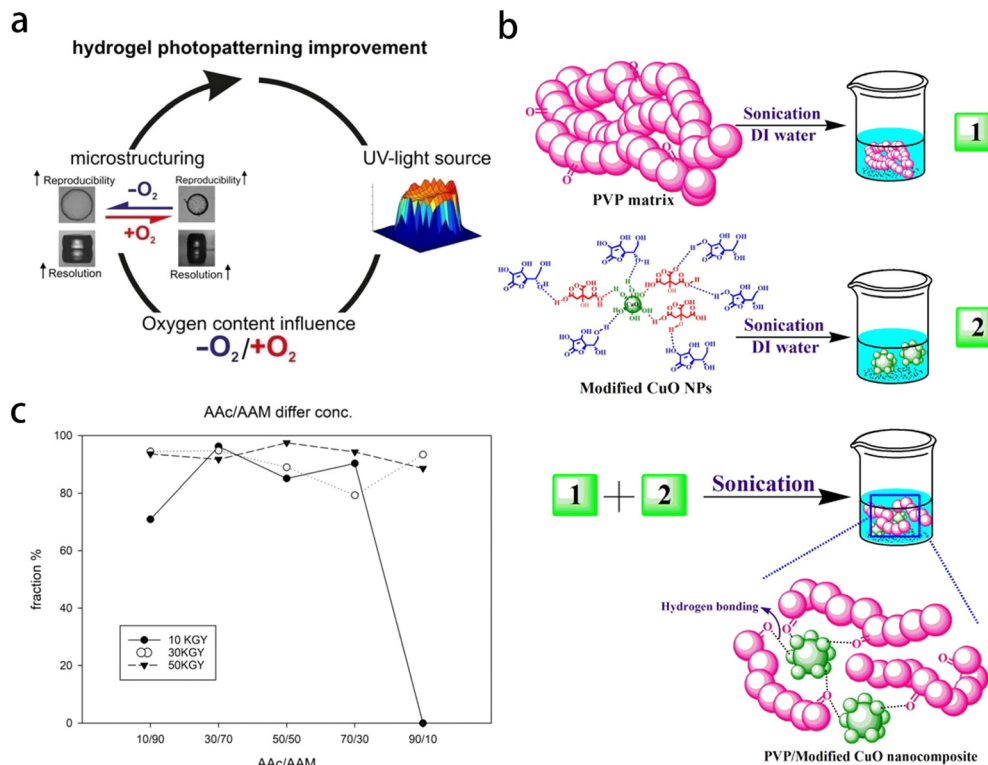


Fig. 2 Gels synthesized by different methods. (a) Poly-*N*-isopropylacrylamide (pNIPAAm) hydrogels photopatterning improvement. Reprinted with permission from ref. 64 (b) preparation of PVP/Modified CuO NC. Reprinted with permission from ref. 65 (c) different radiation dose and composition of AAc/Aam. Reprinted with permission from ref. 66.

gels. (2) It can be divided into single-component gel, two-component gel and multi-component gel according to the components of the contained substances. (3) Depending on the types of gelling agents, they can be divided into aliphatic derivatives, steroid derivatives, nucleoside base derivatives, amino acid and peptide derivatives, carbohydrate derivatives, organometallic complexes, conjugated  $\pi$  systems and more. Supramolecular polymer gel possesses unique mechanical properties, including controllable mechanical strength, viscoelasticity, self-healing and so on. Self-assembled supramolecular polymer gel also has excellent responsiveness to various stimuli (Fig. 3a and b).<sup>70,71</sup> Scanning electron microscope (SEM) has been employed to observe the xerogel of supramolecular polymer, revealing a porous structure that contributes to the observed gelation extension and interconnection (Fig. 3c). In addition, a layered network with holes has been observed (Fig. 3d), demonstrating the diversity of microstructure of supramolecular polymer gel. The mechanical properties of these supramolecular polymer gels can be controlled by changing external stimuli (Fig. 3).

### 3.3 Metal-organic framework gel

Metal-Organic Frameworks (MOFs) are porous materials with a periodic structure, which are formed by self-assembly of central metal ions or clusters and organic ligands. MOFs possess excellent characteristics, including high surface area and porosity, adjustable pore shape and size, adjustable structure,

biodegradability and variable internal characteristics.<sup>72</sup> The polarized surface of MOFs particles is composed of central metal and carboxyl or imidazole groups (Fig. 4), which can interact with hydrophilic polymers in hydrogel and further enhance the mechanical properties of hydrogel. An example is the synthesis of a cobalt catalyst embedded within nitrogen-doped graphene aerogel (Co-N-GA), achieved through a simple *in situ* hydrothermal assembly and pyrolysis method using MOFs@GA composite (Fig. 4a and b). The catalyst exhibits hierarchical pores of micropores, mesopores and macropores, resulting in excellent electrocatalytic performance, high activity and enhanced stability.<sup>73</sup> Another instance involves the formation of various MOF hydrogels (MA-M) by chelating  $\text{Co}^{2+}$  with alginate and 2-methylimidazole. The microstructure of these hydrogels transit from a smooth surface similar to alginate gel to a uniform granular structure.<sup>74</sup>

In recent years, polysaccharide/MOFs composite aerogel materials have been widely used in the fields of adsorption, separation, catalysis, and drug loading. These materials combine the renewable nature and degradation capabilities of polysaccharide aerogels with the advantageous properties of MOFs, including good biocompatibility, strong structural designability, large specific surface area and abundant pores. The types of MOFs involved in polysaccharide/MOFs composite aerogels are relatively focused, such as ZIFs and Zr-based MOFs (Fig. 5). For instance, cellulose/ZIF-8 composite aerogel has good adsorption performance and reusability for common



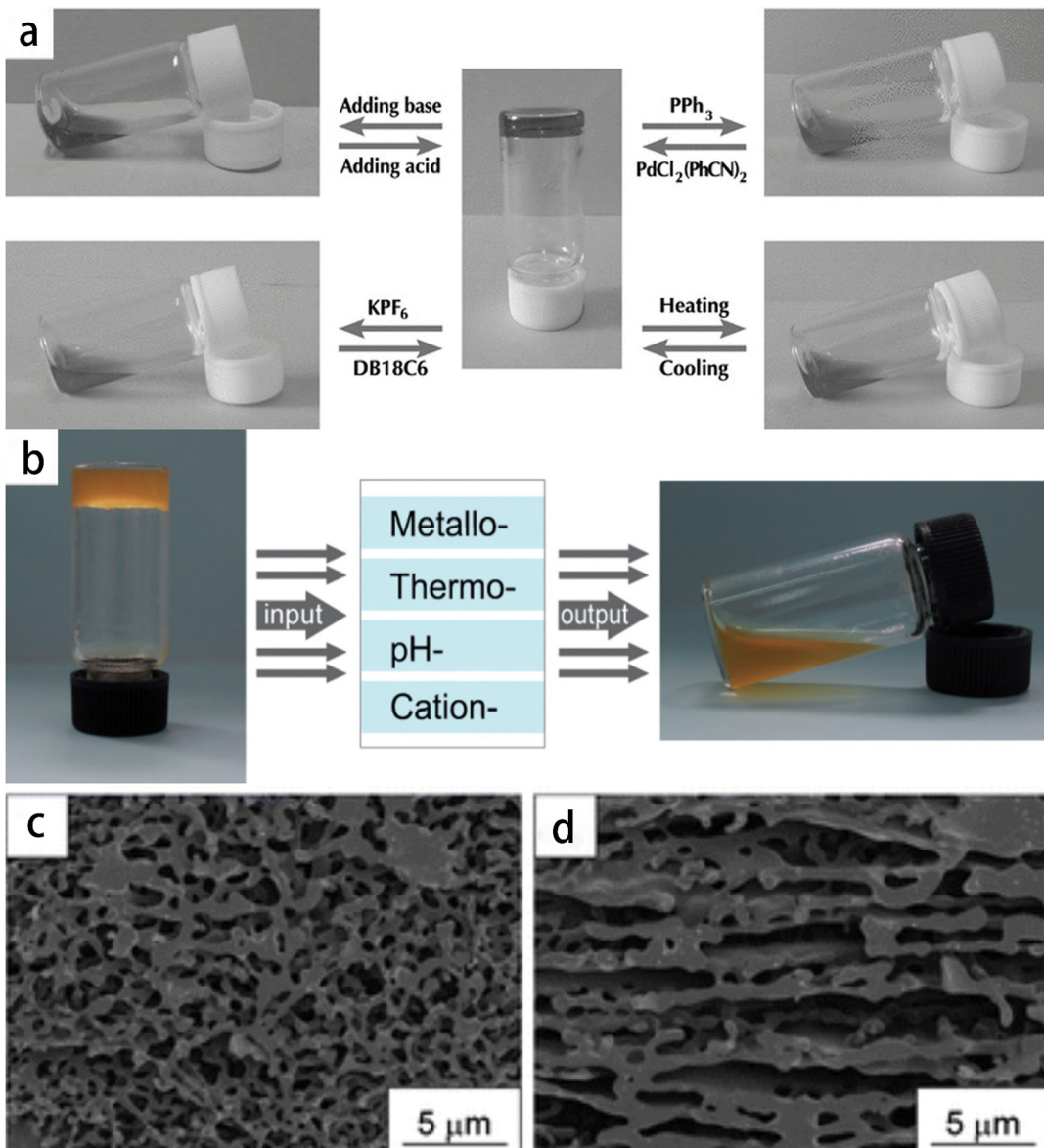


**Fig. 3** The mechanical properties of supramolecular polymer gel are controlled by altering external stimuli. (a) The reversible gel–sol transitions of the supramolecular polymer network gel (50 mM of monomer 1) triggered by four different stimuli (pH-, thermo-, cation-, and metallo-induced). Reprinted with permission from ref. 70 (b) the reversible gel–sol transitions of the metallo-supramolecular polymer network triggered by different stimuli. Reprinted with permission from ref. 71 (c) and (d) SEM images of the metallo-supramolecular polymer xerogels. Reprinted with permission from ref. 71.

organic solvents such as bromobenzene, benzene, dichloromethane, chloroform, tetrachloromethane, ethanol, toluene, cardanol and pump oil.<sup>75</sup> Additionally, through solvent-assisted ligand exchange (SALE) processing, the crystallinity, porosity, and superparamagnetism of the mercapto functionalized magnetic Zr-MOF (MFC-S) are effectively maintained.<sup>76</sup>

## 4. Gels for diagnostics and therapy of respiratory diseases

As a new functional material, gels are widely used in the diagnosis and treatment of respiratory diseases due to their high water absorption capacity and excellent biocompatibility.

Currently, they are primarily utilized in all aspects of imaging diagnosis, etiological diagnosis of infection, and pathological diagnosis. Moreover, gels play a crucial role in surgical procedures, interventional therapies for respiratory diseases, radiotherapy of lung cancer, as well as and drug delivery and release applications.

### 4.1 Diagnostics

**4.1.1 Detection of pathogens.** Metagenomic sequencing, mass spectrometry and other methods are often used to identify pathogens in pulmonary infectious diseases. These detection techniques often involve polyacrylamide gel electrophoresis or agarose gel electrophoresis (Fig. 6). Polyacrylamide gel is a

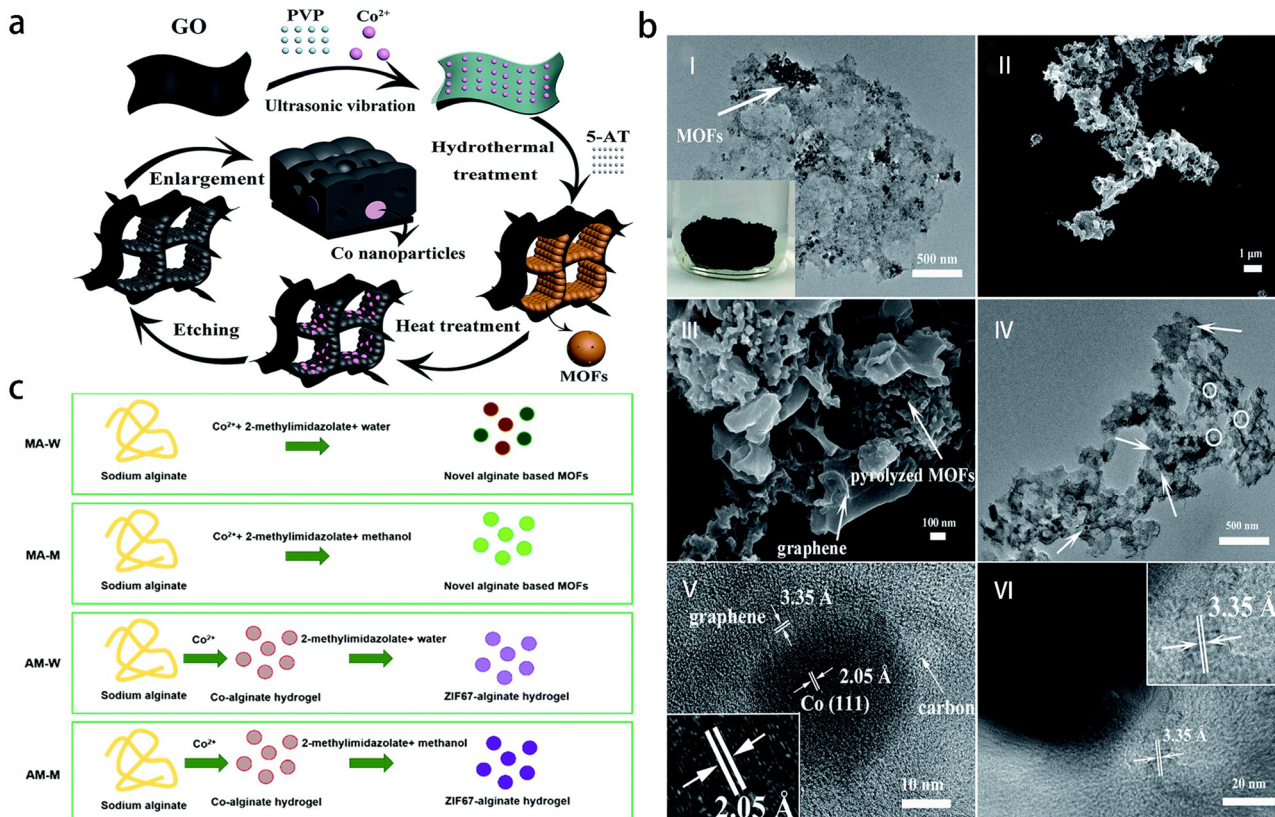


Fig. 4 Preparation procedures of diverse metal–organic framework gel. (a) Illustration of the preparation procedure of Co-N-GA. Reprinted with permission from ref. 73 (b) (I) TEM of MOFs@GA; the inset shows the photograph of MOFs@GH, (II and III) SEM and (IV–VI) TEM of Co-N-GA. Reprinted with permission from ref. 73 (c) schematic illustration of the preparation routines for the alginate-MOF hydrogels. Reprinted with permission from ref. 74.

three-dimensional network gel formed by polymerization and cross-linking of acrylamide (Acr) and cross-linking agent *N,N'*-methylene bisacrylamide (Bis) under the action of ammonium persulfate (AP), *N,N',N'*-tetramethylethylenediamine (TEMED), and electrophoresis is carried out with this as a support. Through polyacrylamide gel electrophoresis, proteins can be separated into distinct bands based on their varying electric charge and molecular size. SDS, an anionic surfactant, disrupts the hydrogen bond and hydrophobic bond of protein, forming short rod-shaped compounds with uniform density when combined with protein molecules in specific proportions. The length of the compounds correlates positively with the molecular weight of the protein. Polyacrylamide gel is transparent, elastic and processes favourable mechanical properties. Additionally, the pore size of the gel can be adjusted. The pore size of the gel can be customized by selecting an appropriate gel concentration based on the molecular weight of the target substance and by modifying the concentration of monomers and cross-linking agents.<sup>77</sup>

Agarose gel electrophoresis is an electrophoresis method using agar or agarose as the supporting medium. It is particularly suitable for samples with larger molecular weights, such as macromolecular nucleic acids and viruses. For efficient separation, agarose gels with larger pore sizes are typically used. Agarose gel is known for its safety and ease of operation.

In this specific system, histidine/2-(*N*-morpholino) ethanesulfonic acid (His/MES) with pH of 6.1 was used as buffer. Within this system, the migration of molecules occurs based on their isoelectric point (PI). Basic molecules with isoelectric point (PI) higher than 6.1 migrate to the cathode, while acidic molecules migrate to the anode. This characteristic allows for the analysis of proteins in their natural (non-denatured) state regardless of PI.<sup>78</sup> Thus, the small differences in structural properties among SARS-CoV-2 mutants can be detected.<sup>79</sup>

**4.1.2 Pathological diagnosis.** CT-Guided percutaneous lung puncture is a highly reliable and accurate method for diagnosing lung diseases. As the incidence of lung cancer continues to rise and the detection rate of asymptomatic pulmonary nodules increases, there is a growing demand for lung biopsies that involve new molecular profiling and genomic analysis of the tissue. In this context, more and more gel materials are used in CT-guided percutaneous lung puncture (Fig. 7). A most common complication associated with this procedure is pneumothorax. The use of an artificial hydrogel plug called BioSentry significantly has reduced the incidence of pneumothorax in patients undergoing CT-guided lung biopsies, as well as reduced rates of chest tube placement and postoperative hospitalization.<sup>80</sup>

The implementation of lung cancer screening programs has significantly increased the detection rate of sub-centimeter lesions, including solid masses and ground glass opacity



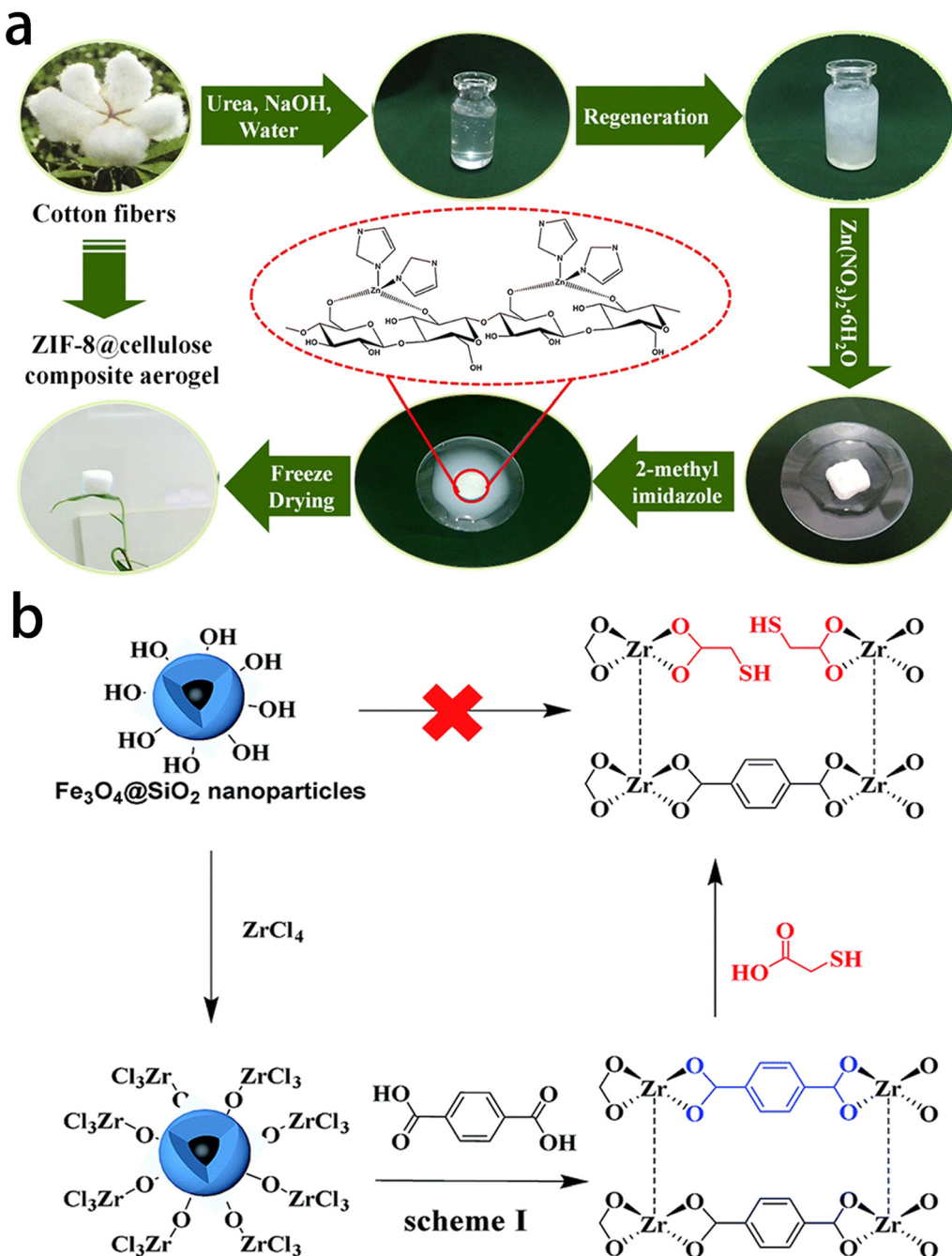


Fig. 5 Synthesis of the polysaccharide/MOFs composite aerogels. (a) Diagrammatical illustration of synthesis of the ZIF-8@cellulose composite aerogels. Reprinted with permission from ref. 75 (b) schematic diagram of the preparation of MFCs. Reprinted with permission from ref. 76.

(GGO) sub-centimeter lesions. As a result, there is a growing need for histological diagnosis in these cases. While a percutaneous CT-guided biopsy can be challenging, surgical excision is an effective diagnostic option. CT-guided hydrogel plug deployment (BioSentry<sup>®</sup>) has recently been proposed to simplify intraoperative nodule localization (Fig. 7b–e). CT-Guided hydrogel plug placement can successfully detect GGOs in the lung and resect GGOs by the uniVATS approach. This equipment facilitates the diagnosis of lung cancer and achieves successful treatment in 85.4% of cases.<sup>81</sup>

**4.1.3 Imaging diagnosis.** Synthetic hydrogel particles based on polymers provide the flexibility to combine targeted peptides with imaging probes and encapsulate diagnostic and therapeutic agents for delivery to the lungs (Fig. 8). Brody *et al.* designed polyacrylamide hydrogel particles with different sizes and functionalized them with non-arginine cell penetrating peptide (Arg9, Fig. 8a–c). Through the evaluation of model particles, it was found that larger polyacrylamide microparticles (PMP) exhibited a brief residence time in the airways and were rapidly cleared through the gastrointestinal tract, potentially *via* the mucociliary pathway.

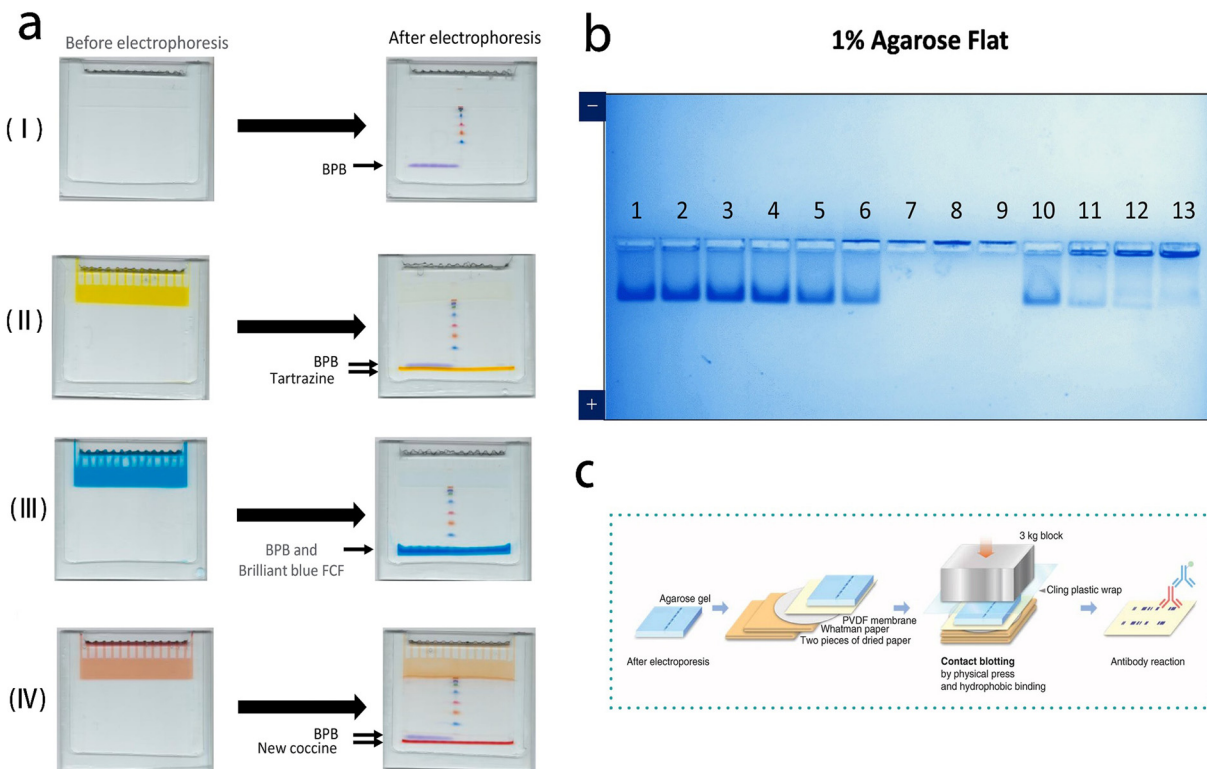


Fig. 6 Polyacrylamide gel electrophoresis and agarose gel electrophoresis for pathogen detection. (a) Standard (stacking gel without dye) (I) and improved electrophoreses (stacking gel with dye) (II–IV). Reprinted with permission from ref. 77 (b) agarose native gel electrophoresis of heat- and acid-treated virus. Reprinted with permission from ref. 78 (c) schematic illustration of contact blotting procedure. Reprinted with permission from ref. 79.

Their half-life in the lungs was also very short. These particles, when lacking cell penetrating peptide (CPP) Arg9, did not cause acute inflammation. Therefore, they can be used for diagnostic imaging of conditions requiring relatively short lung residence time, such as acute lung injury (including acute lung infection and acute respiratory distress syndrome). On the other hand, smaller polyacrylamide nanoparticles (PNP) demonstrated a longer retention time and a higher retention rate in the lung membrane, which was further increased by Arg9. However, no acute lung inflammation was observed with these nanoparticles. Therefore, these nanoparticles may be more suitable for continuous imaging purpose.<sup>82</sup>

#### 4.2 Therapy

The treatment of respiratory diseases primarily depends on the etiology and associated clinical symptoms. Drug therapy plays a crucial role in the treatment of most pulmonary infectious diseases, encompassing various administration routes such as oral, intravenous, and atomized inhalation. Furthermore, the selection of chemotherapy, radiotherapy, surgery or interventional therapy depends on individual circumstances. Along with the rapid development of gel technology, gel-based nano-composites have been widely used in the treatment of respiratory diseases.

**4.2.1 Surgery and interventional therapy for respiratory diseases.** Surgery and interventional therapy are important methods in the treatment of respiratory diseases (Fig. 9).

Among these, cryosurgery stands out as a minimally invasive technique that uses freezing temperatures to eradicate tissues for the treatment of various diseases, including lung cancer.<sup>83</sup> The main advantage of cryosurgery is that it cryosurgery offers the advantage of targeting a substantial volume of tissue while preserving the surrounding structures to a large extent. Cryosurgery reduces the risk and shortens the recovery time compared to certain traditional operations.<sup>84</sup> However, it encountered some challenges in practical use, partly due to the difficulty in predicting treatment outcomes. To address this issue, Michael L. and colleagues proposed the application of predictive modeling ultrasonic gel, which has temperature-dependent thermal characteristics, serves as a convenient tissue membrane (Fig. 9a). The temperature inside and around the “ice ball” was plotted by carefully placing thermocouple arrays in the ultrasonic gel, which characterized the freezing situation around the single and two interacting freezing probes.<sup>85</sup>

With the advancement of chest CT and imaging technology, the incidence of lung nodules has been increasing. Accurate segmentation of lung nodules in chest CT images is crucial for image-guided lung cancer diagnosis and treatment planning.<sup>86</sup> When lung cancer is highly suspected, many patients opt for video-assisted thoracic surgery (VATS) as a treatment option. VATS is becoming increasingly popular for partial resection of lung nodules due to its minimally invasive nature compared to thoracotomy.<sup>87</sup> However, locating small or ground-glass



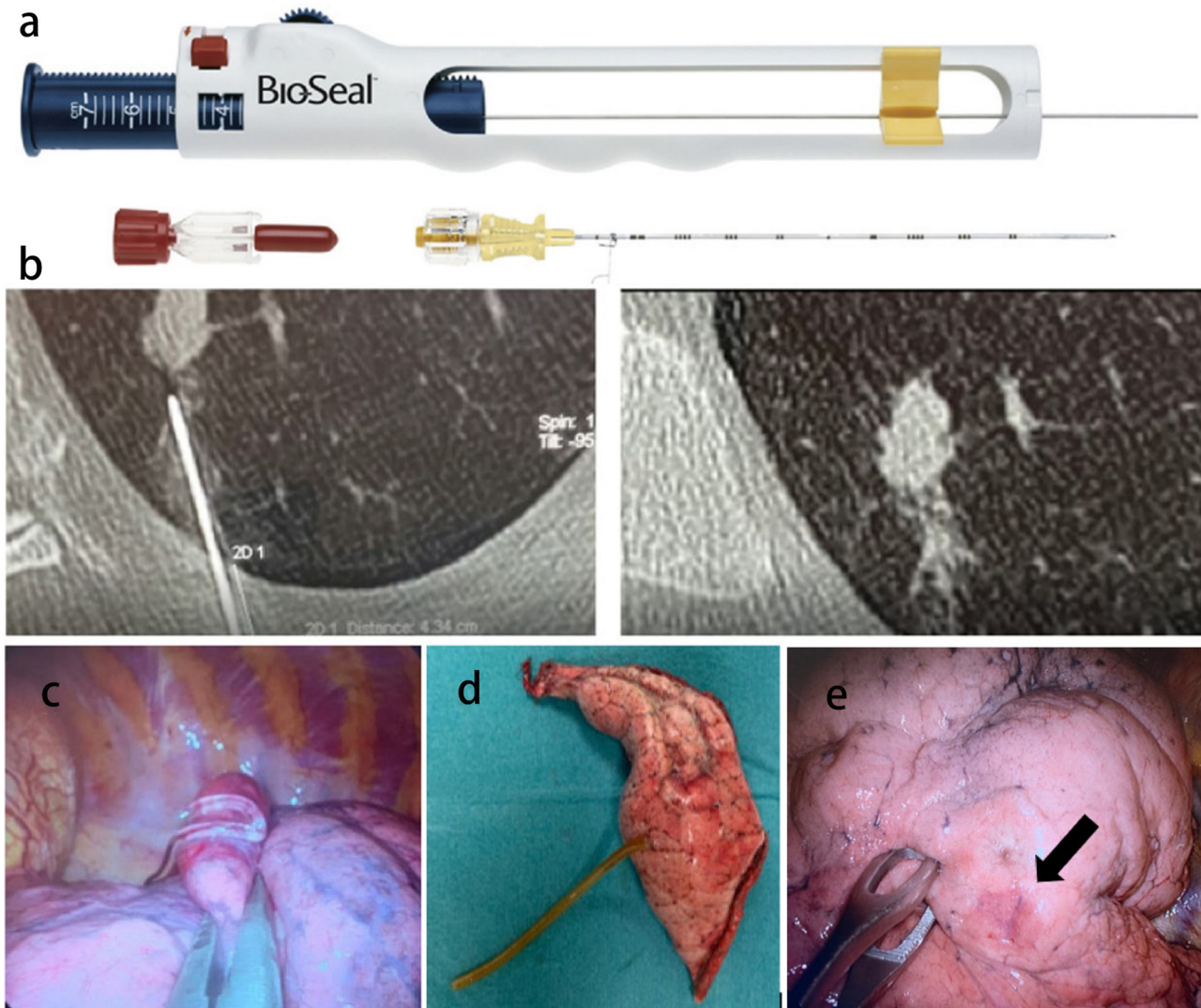


**Fig. 7** Application of gel material in CT-guided percutaneous lung puncture. (a) The Bio-Seal Lung Biopsy Tract Plug. Reprinted with permission from ref. 80 (b) a CT scan showing the plug deployment. (c) Hydrogel plug sealed into lung parenchyma (uniVATS vision). Reprinted with permission from ref. 81 (d) lung specimen with hydrogel plug previously deployed (1 month before surgery). (e) A case of hydrogel plug dislodgment. The arrow indicates the subpleural suffusion nearby the percutaneous lung puncture. Arrow: outlines the subpleural suffusion. Reprinted with permission from ref. 81.

opaque nodules before VATS are difficult.<sup>88</sup> Therefore, various percutaneous positioning techniques are used to aid in localization before the surgery. These techniques include short hook wire placement,<sup>89</sup> radionuclide injection,<sup>90</sup> contrast agent injection such as lipiodol or barium,<sup>91</sup> dye injection,<sup>92</sup> and so on. Studies have shown the feasibility of using the mixed labeling of indigo carmine, lipiodol and lidocaine gel before operation. Lidocaine gel, as a surfactant, forms micelles and connect oil-based lipiodol with water-soluble indigo carmine. Lidocaine gel also increases the viscosity of the mixture, preventing the dye from spreading to the lung.<sup>93</sup>

Pneumothorax is a common complication following thoracoscopic lung nodule resection. Various biological and synthetic materials have been used to seal the resected lung tissue to solve this problem, but their effectiveness has been limited. PleuraSeal is a novel, 100% synthetic, and biodegradable

hydrogel, which can eliminate the risks of allergic reaction, immune reaction and virus transmission. As an inert substance, PleuraSeal does not support the growth of bacteria, and it does not contain latex, making it safe for patients with latex allergies. The gel consists of two liquid components: polyethylene glycol ester (PEG) and tri-lysine amine (Fig. 9c). PEG, the first component, is a water-soluble, non-toxic and biocompatible component with active bonds. PEG is provided in the form of transparent blue solution, and imparts a blue color to the polymerized hydrogel. The second component, tri-lysine, is derived from *L*-lysine, which is obtained through the fermentation of sugarcane molasses or tapioca starch. While tri-lysine is derived from plants, the final product is considered to be synthetic. PleuraSeal can be used as a spray to seal lung tissue after thoracoscopic resection and also as a preventive adjuvant for thoracoscopic lung surgery.<sup>94</sup>

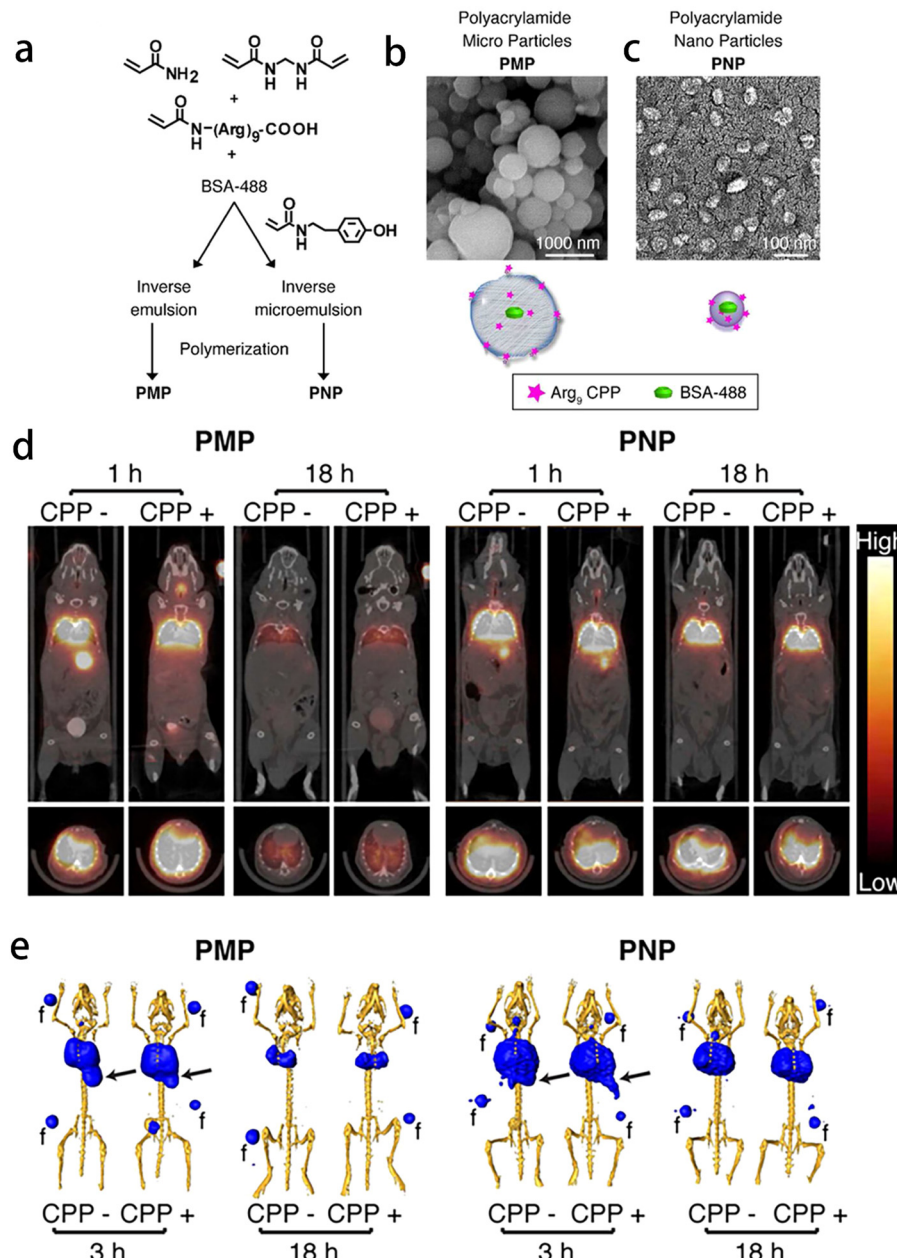


**Fig. 8** Application of gel materials in imaging diagnosis of respiratory diseases. (a)–(c) Synthesis, functionalization, and *in vitro* behavior of polyacrylamide hydrogels. Reprinted with permission from ref. 82 (d) and (e) MicroPET/CT imaging of <sup>76</sup>Br-labeled particles following intratracheal delivery. Reprinted with permission from ref. 82.

Hemoptysis one of the most common acute and severe diseases of respiratory system, and severe hemoptysis can lead to suffocation and death of patients. Bronchial artery-pulmonary artery fistula represents an abnormal vascular connection between systemic and pulmonary circulations, leading to increased blood flow in the bronchial artery, which can cause rupture and bleeding. This condition is a common contributor to recurrent refractory hemoptysis. Bronchial artery embolization is the primary treatment choice for managing this type of massive hemoptysis. There are many embolic materials that can be used for interventional therapy, with the gelatin sponge

strip being the most commonly used in clinical practice. The gelatin sponge strip offers advantages such as absence of antigenicity, disinfection and cost-effectiveness. However, it is prone to blood vessel recanalization. In recent years, GU *et al.* proposed a new concept of vascular embolization involving controllable aggregation of colloidal hydrogel microspheres. With this strategy, solid embolism of fluid-like injection can be achieved. Colloidal microspheres not only have the function of embolization, but also have the potential functions such as hyperthermia, drug loading and CT imaging. Therefore, magnetic polyvinyl alcohol hydrogel microspheres were synthesized



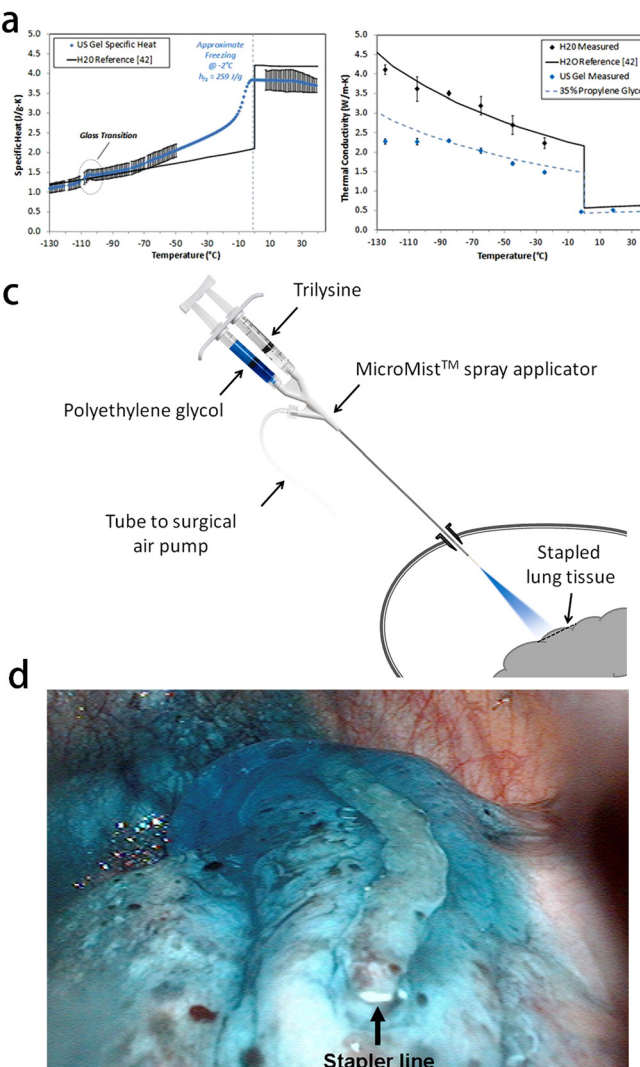
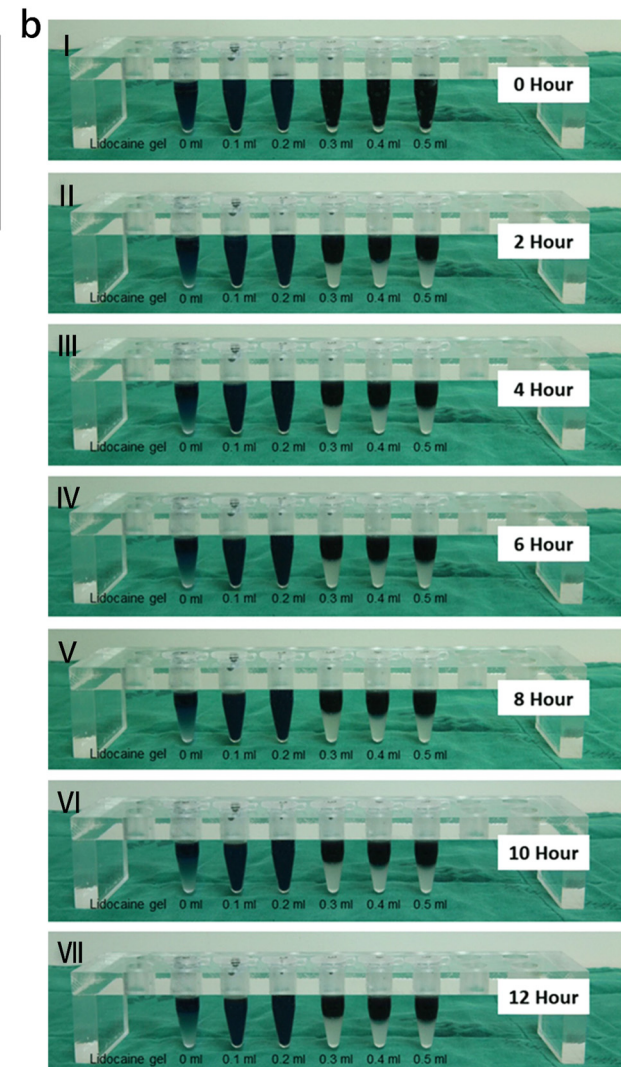


**Fig. 9** Application of gel in surgical operation and interventional therapy of respiratory diseases. (a) Measured ultrasound gel specific heat (left) and thermal conductivity (right). Reprinted with permission from ref. 85 (b) changes over time in mixtures containing indigo carmine, lipiodol and lidocaine gel. Reprinted with permission from ref. 93 (c) the PleuraSeal lung sealant system. The 2 components, polyethylene glycol and tritylamine, are sprayed with the MicroMist spray applicator, which is attached to a surgical air pump. The applicator can be passed through a port, and the tip is positioned at a distance of 2 cm from the tissue site to be sealed. Reprinted with permission from ref. 94 (d) thoracoscopic view of the transparent blue seal after spray application of PleuraSeal lung sealant at the site of pulmonary tissue resection (with an endoscopic linear stapler). Reprinted with permission from ref. 94.

by inverse suspension crosslinking method. In the presence of magnetic field, the microspheres could be controlled to aggregate within the fluid. Magnetic hydrogel microspheres possess the special fluidity of iodized oil and can form solid operators, so they are expected to be widely used in clinical vascular embolization in the future.<sup>95</sup>

**4.2.2 Radiotherapy of lung cancer.** Radiation therapy is a common treatment for lung cancer, and the use of gel plays a significant role in the process (Fig. 10). With the development of dynamic radiotherapy technologies, such as Tomo therapy, arc-controlled radiotherapy and intensity-modulated radiotherapy, radiotherapy technologies are becoming more and more complex, making quality assurance and control of radiotherapy schemes of paramount importance. Therefore, metrological verification before treatment is the key part to ensure



quality and control. Accurate metrological verification not only effectively reduce the risk of errors in radiotherapy but also minimize side effects and recurrence rate of radiotherapy.<sup>96</sup> In 1984, Gore *et al.* proposed the concept of 3D chemodosimetry, which used gel matrix with Fricke dosimeter to measure dose distribution with the aid of magnetic resonance imaging (MRI).<sup>97</sup> The 3D metrology has developed rapidly in recent years. This includes the use of polymer gel dosimeter (Fig. 10a) dosimeter using oxygen scavenger and other dosimeters based on radiochromic reaction.<sup>98</sup> The 3D lung simulation dosimeter has also been proposed to address the limitations of traditional gel formulations, which are typically water-equivalent and not ideal for measuring dose in lung tissue. To reduce the density of gel, there are two common methods: foaming the gel before solidification and incorporating

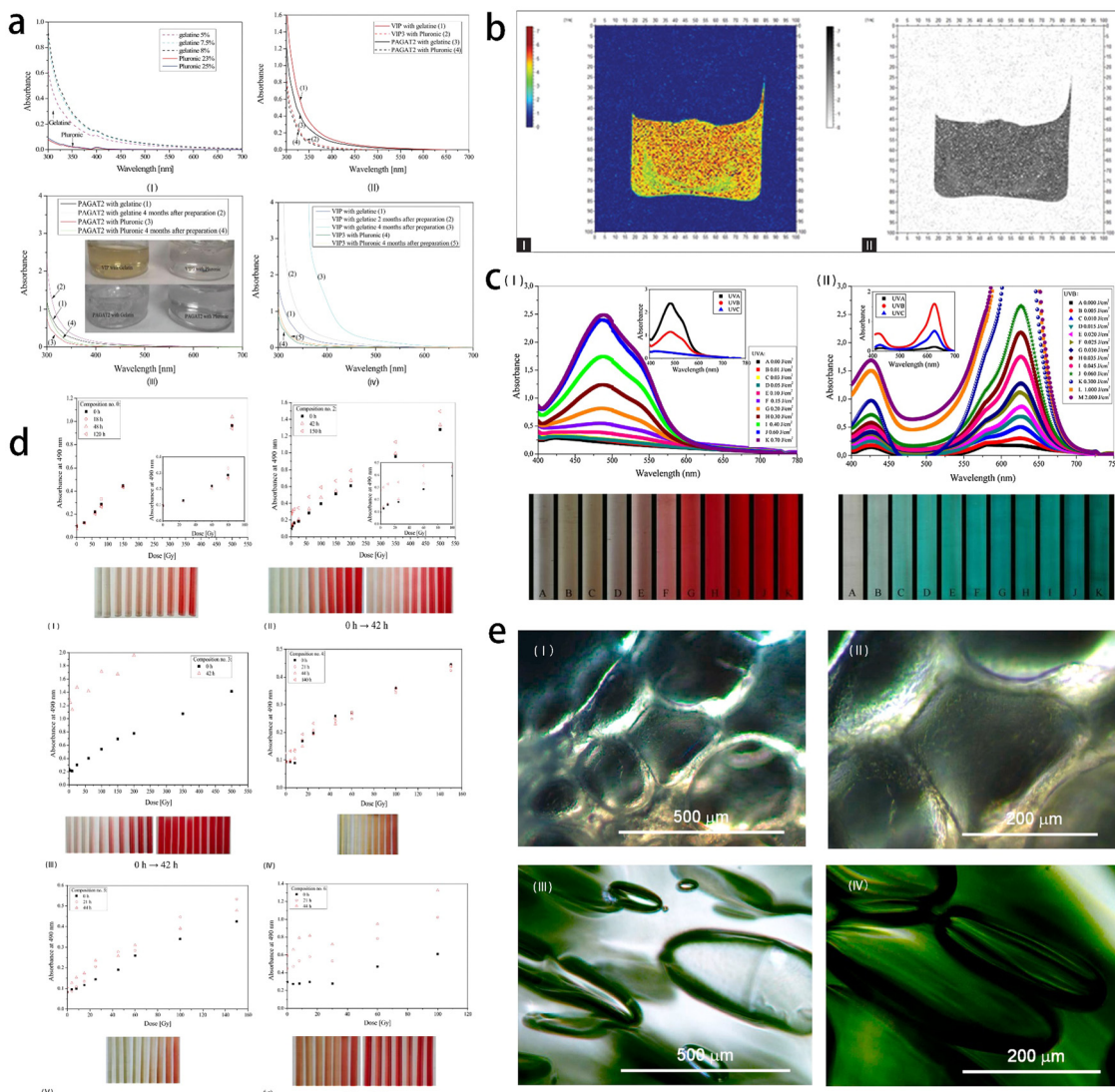


**Fig. 10** Application of gel in radiotherapy of lung cancer. (a) Optical properties of five 3D radiotherapy polymer gel dosimeters. Absorbance spectra of non-irradiated (I) pluronic and gelatine physical gels, and (II) PAGAT2 containing a gelatine and pluronic gel matrix, VIP containing a gelatine matrix and VIP3 containing a Pluronic matrix. (III) A comparison of the UV-Vis spectra of non-irradiated PAGAT2 containing a gelatine and Pluronic matrix immediately after preparation and four months after preparation. (IV) A comparison of the UV-Vis spectra of VIP containing a gelatine matrix immediately after preparation and two and four months after preparation, and VIP3 containing a Pluronic matrix immediately after preparation and four months after preparation. Reprinted with permission from ref. 98 (b) color R2-map and R2-map inverted gray scale obtained lung-equivalent gel from magnetic resonance imaging scanning. Reprinted with permission from ref. 99 (c) UV dose response spectra of TTC- (I) and LMG-Pluronic (II) gels. Reprinted with permission from ref. 100 (d) stability over time of TTC-Pluronic gel compositions. Reprinted with permission from ref. 101 (e) (I-II): a view under a microscope of PAGAT-2-Pluronic F-127 gel dosimeter mimicking lungs; (III-IV) correspond to the same dosimeter, however, with 1 M NaCl (magnification, left:  $\times 10$ , right:  $\times 20$ ). Reprinted with permission from ref. 102.

polystyrene beads to simulate bubbles and enhance surfactant properties. The dose response of gel foam dosimeter to R2 depends on density (Fig. 10b).<sup>99</sup> Recently, a nonionic physical gel-forming poly(ethylene oxide)-block-poly(ethylene oxide)-block-poly(ethylene oxide) copolymer (Pluronic F-127) has been proposed as a UV and matrix for ionizing radiation 3D dosimeters.<sup>100</sup> The ultraviolet dose response spectrum of gel shows that the intensity of color is correlated with the absorbed dose of radiation, with darker color indicating higher doses (Fig. 10c). This gel dosimeter offers several advantages, including

high transparency, wide range of thermal stability (Fig. 10d) (especially at the temperature above 30 °C, where most 3D gel dosimeters based on gelatin matrix can dissolve) non-toxicity, and safety. Moreover, it eliminates the use of gelatin, a natural polymer, in the preparation of 3D dosimeter.<sup>101</sup> At present, Kozicki *et al.* have put forward another new type of simulated lung dosimeter. This dosimeter does not have any additional surfactant in its composition, but only depends on the surface and interfacial activity of Pluronic F-127, which is a copolymer matrix. This new type of dosimeter holds

Table 1 Hydrogel for drug delivery of respiratory diseases

Diseases	Components	Route of administration	Ref.
Lung cancer	AuP loaded IPN	<i>In vivo</i>	103
Lung cancer	PVP/PMASH system	<i>In vitro</i>	104
Lung cancer	Multifunctional RNA nanohydrogels (RNA NHs)	<i>In vivo</i>	105
Lung cancer	PLGA-PEG-PLGA	<i>In vivo</i>	106
Asthma	PLGA-PEG-PLGA	<i>In vivo</i>	107
Pneumonia	Poly(methacrylic acid) hydrogels	<i>In vivo</i>	108
Pleural effusion	Chitosan-SN-hyaluronic acid hydrogel	<i>In vivo</i>	109

great potential for 3D radiation dosimetry in lung tumor eradication.<sup>102</sup>

**4.2.3 Drug delivery and release.** Drug delivery and release play a crucial role in the application of hydrogel for the treatment of respiratory diseases (Table 1). The unique physical properties of hydrogels offer significant advantages for efficient drug delivery, enabling sustained release of encapsulated drugs. Hydrogels can maintain a high local concentration of drugs over an extended period through various release mechanisms, including diffusion, swelling, chemical or other environmental stimuli.

The hydrogel scaffold serves as a localized drug delivery system, which can maintain the therapeutic level of drug concentration in tumor tissue. In this study, a biopolymer hydrogel scaffold coated with adriamycin was prepared using gelatin, sodium carboxymethylcellulose and gelatin/sodium carboxymethylcellulose mixture through freeze-drying. The scaffolds made of different types of natural polymers have different pore configurations and pore sizes. Compared with the control group, the viability and proliferation of A549 cells treated with gelatin, gelatin/SCMC and SCMC scaffolds containing adriamycin decreased significantly. These findings suggest that these hydrogel scaffolds may provide a promising method for developing an improved local drug delivery system for eradicating lung cancer cells.<sup>110</sup>

Gel materials play a significant role in targeted therapy of lung cancer (Fig. 11). Erlotinib (ERT) is one of the most critical targeted drugs for the treatment of non-small cell lung cancer (NSCLC). However, its limited clinical application is attributed to poor solubility, low oral bioavailability and unpredictable toxicity. To overcome these challenges, a novel injectable matrix was developed using hollow mesoporous silica nanoparticles (HMSNs) and thermosensitive poly(D,L-lactide)-poly(ethylene glycol)-poly(D,L-lactide) (PDLLA-PEG-PDLLA, PLL) hydrogel. This matrix enables the sustained release of ERT, enhancing its therapeutic efficacy against NSCLC (Fig. 11a). Test tube inversion method showed that the ERT-loaded hydrogel composite (ERT@HMSNs/gel) presented as an injectable flowing solution at room temperature, and changed into a physically crosslinked non-flowing gel structure at physiological temperature. *In vivo* imaging studies showed that ERT@HMSNs/gel complex showed prolonged drug retention time in and around the tumor. This new ERT-loaded HMSNs/gel system shows promise as an *in situ* treatment for non-small cell lung cancer and offers a promising platform for the design and preparation of nano-drug delivery system for local anticancer therapy.<sup>111</sup> KRAS mutation represents a significant subtype of lung adenocarcinoma. The clinical approach for this subtype is chemotherapy. However, conventional chemotherapy fails to

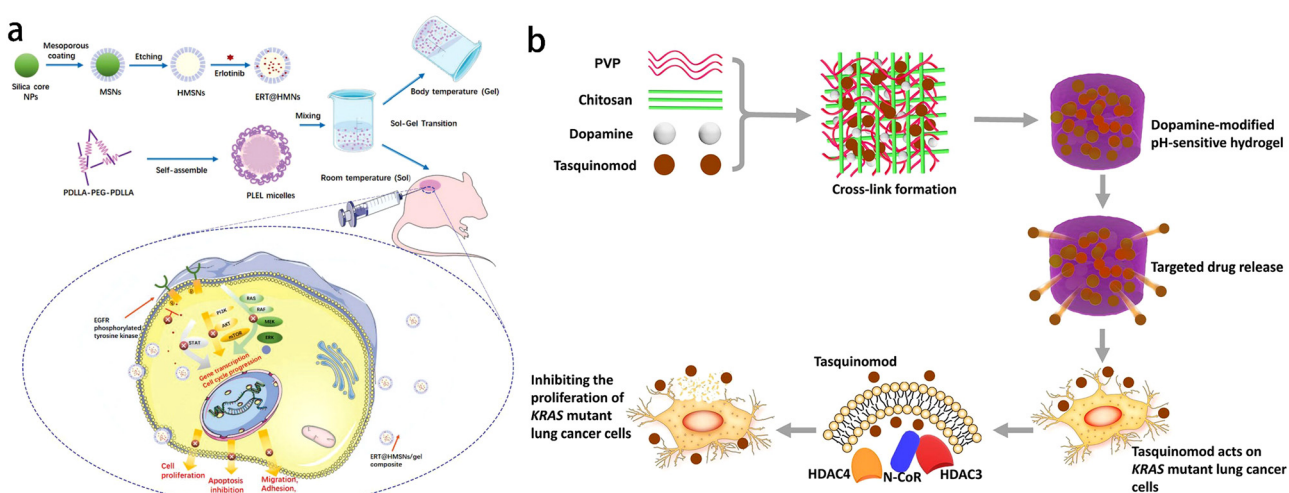


Fig. 11 Application of gel in drug release for treating lung cancer. (a) Schematic representation of the ERT@HMSNs and ERT@HMSNs/gel composite. HMSNs/gel *in situ* drug delivery platform was employed for localized and sustained delivery of small molecule, erlotinib, to promote its therapeutic efficacy and ameliorate drug-related toxicity. Reprinted with permission from ref. 111 (b) schematic diagram of dopamine-modified pH sensitive hydrogel which is effective at inhibiting the proliferation of KRAS mutant lung cancer cells. Reprinted with permission from ref. 112.



ensure a high drug concentration at the tumor site, necessitating frequent injections to maintain effective drug levels. The pH sensitive hydrogel developed by Sang *et al.* is based on polyvinylpyrrolidone (PVP) and chitosan, with the addition of dopamine to enhance its gelation and support properties. The incorporation of dopamine enables faster solidification of the crosslinked hydrogel compared to the alkaline hydrogel while maintaining its pH sensitivity. Tasquinimod can inhibit the proliferation of KRAS mutant lung cancer cells, and this inhibitory effect is enhanced when combined with PVP-chitosan dopamine pH-responsive hydrogel system (Fig. 11b). This novel approach utilizing biomaterials for treating KRAS mutant lung cancer offers advantages such as increased efficiency and reduced side effects, presenting a new way for clinical treatment.<sup>112</sup>

Administration through pulmonary route offers the advantage of increasing local drug concentration in the lungs, thereby improving the local antibacterial effect of pulmonary infection. In the case of conditions such as cystic fibrosis and pneumonia, reducing the frequency, dose and duration of inhalation therapy can improve the compliance of patients.

The utilization of sustained-release preparations is a promising approach to prolong the residence time of drug-releasing particles in the lungs and decrease the frequency of inhaled aerosol administration (Fig. 12). However, there are few effective sustained-release lung preparations developed at present, as the inhaled particles can be effectively removed by mucociliary automatic clearance or alveolar macrophage uptake. Ibrahim *et al.* synthesized a copolymer (PEG-g-PHCs) of polyethylene glycol grafted onto benzoyl chitosan, and self-assembled with ciprofloxacin to form drug-loaded nanoparticles. Nanoparticles and free drugs are encapsulated in breathable and expandable alginate hydrogel particles, creating a novel continuous lung drug delivery system. The self-assembled ciprofloxacin nanoparticles were then encapsulated in dry expandable nano-microgel particles without  $\text{Ca}^{2+}$ . The preparation has good aerodynamic characteristics and sustained-release characteristics. When administered to rats, ciprofloxacin achieved lower systemic exposure while maintaining a higher concentration in the lungs for over 7 hours. This approach provides a new way to treat pulmonary infectious diseases by pulmonary route.<sup>113</sup>

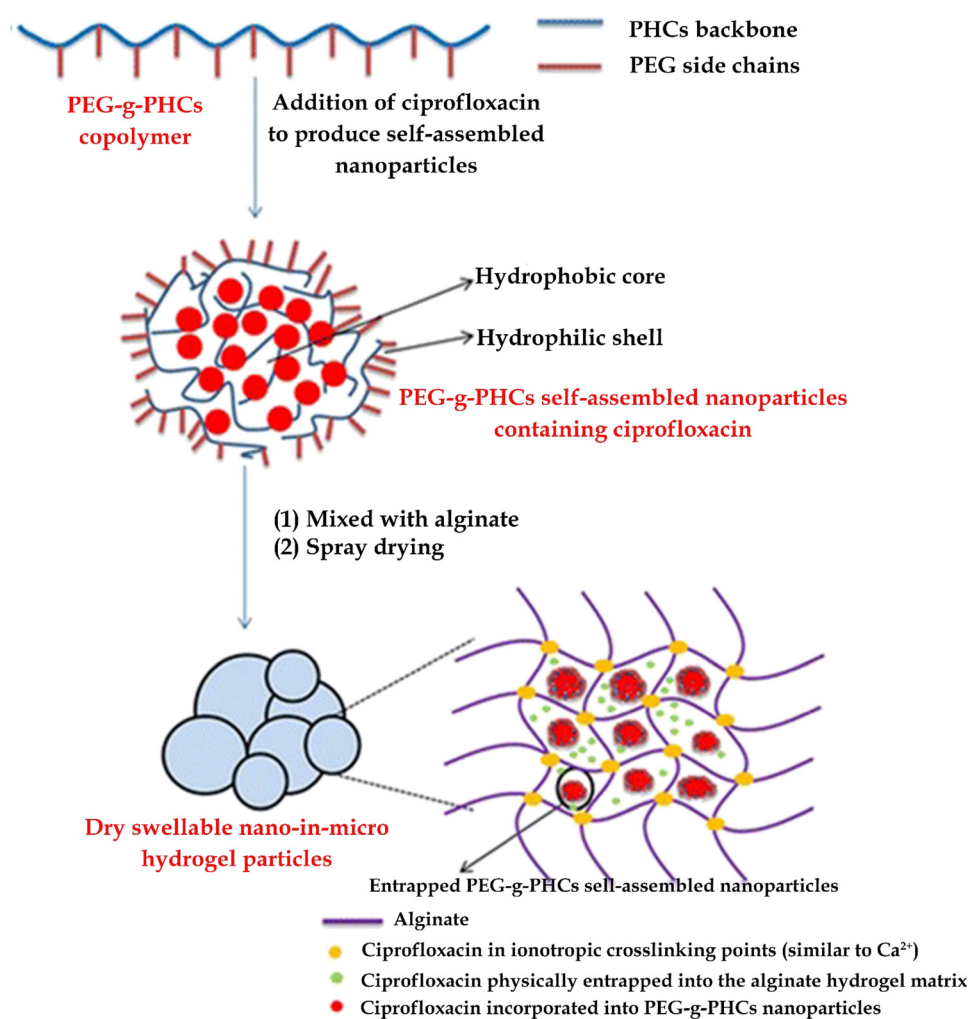


Fig. 12 A novel antibiotic hydrogel particle with high drug loading has been formed to achieve controlled pulmonary drug delivery. Reprinted with permission from ref. 113.



Empyema is an inflammatory disease affecting the pleura, characterized by the accumulation of pus in the thoracic cavity, usually accompanied by bacterial pneumonia. During the disease progression, pro-inflammatory and pro-fibrogenic cytokines in suppurative pleural effusion stimulate fibroblast proliferation and extracellular matrix deposition, leading to fibrin deposition and formation of fibrothorax. Treatment of encapsulated empyema commonly involves the infusion of urokinase through a thoracic drainage tube. However, the frequent administration of urokinase (2–3 times a day, lasting 4–8 days) is required. Due to its high-water solubility, urokinase is easy to flow out of the thoracic drainage tube. In an *in vitro* study, a thermos responsive hydrogel based on poloxamer 407 (P407) and hyaluronic acid (HA) was developed to optimize the loading and release of urokinase. The hydrogel system composed of P407 and HA has excellent performance in slowing down gel erosion and improving hydrogel performance, providing higher swelling performance, more compact microstructure and smaller pore size. Importantly, the hydrogel did not exhibit cytotoxicity upon local injection, ensuring safety. The developed hydrogel has successfully achieved sustained release of urokinase for 24 hours, making it a promising material for loading hydrophilic drugs in the future.<sup>114</sup>

IPF is a life-threatening disease characterized by progressive pulmonary fibrosis, leading to chronic respiratory failure and severe hypoxemia. The key histological feature of IPF is the excessive proliferation of fibroblasts, resulting in the accumulation of dense collagen. Current treatment options of IPF include oxygen therapy and anti-fibrosis drugs, such as Nintedanib and Pirfenidone (PDF), which can slow down the progression of disease in the early stages (Fig. 13a). Pirfenidone is widely used for anti-fibrosis treatment. However, oral dosage forms still have certain limitations, including issues related to first-pass metabolism and gastrointestinal irritation. To overcome these limitations, a liposomal formulation containing PDF was developed using soybean phosphatidylcholine (SPC) and sodium cholate (SC) through membrane hydration method. The optimized liposome formula was then added into hydroxypropyl methyl cellulose (HPMC) hydrogel. Penetration enhancers such as oleic acid (OA) and isopropyl myristate (IPM), were added to facilitate the effective absorption of PDF through the skin. Therefore, liposome hydrogel preparation containing PDF can be used as a potential transdermal drug delivery system.<sup>115</sup>

Despite available treatments, the median survival time of IPF patients is short, ranging from 2 to 3 years. In cases of

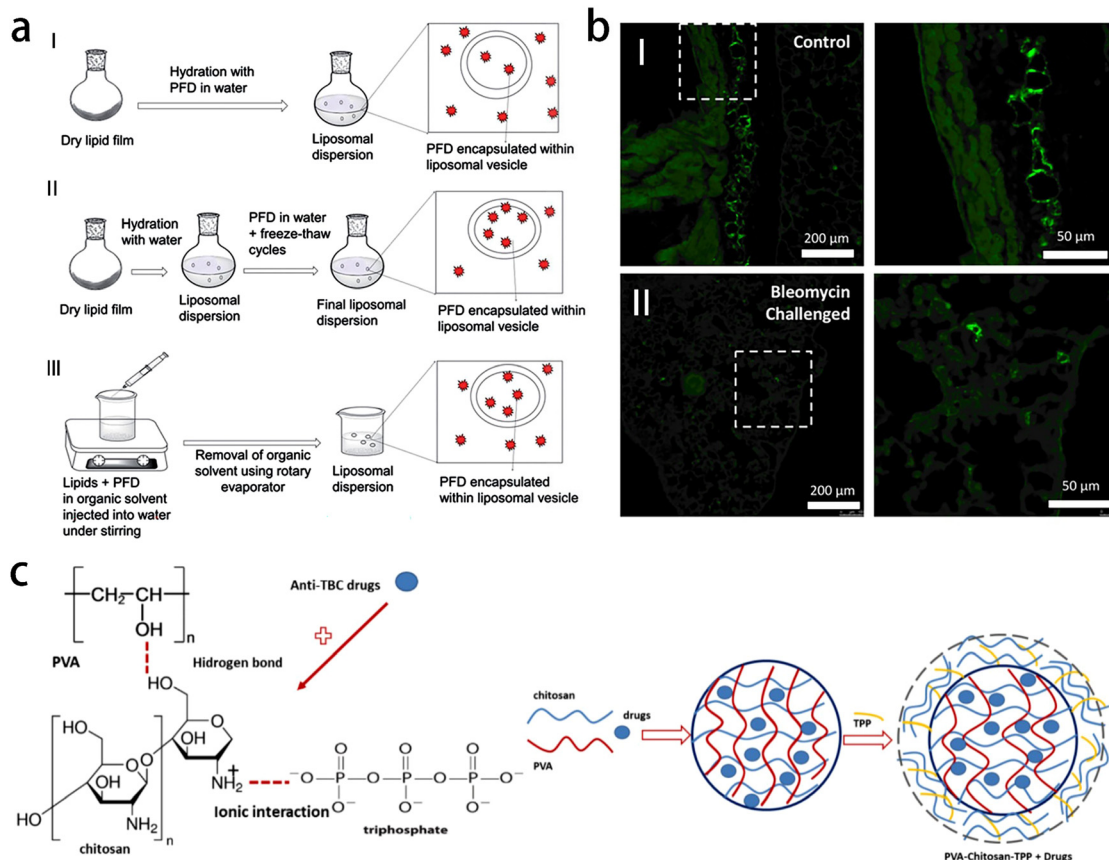


Fig. 13 Applications of gel materials used for the treatment of other lung diseases. (a) Schematic representation of PFD loading in liposomes prepared by thin film hydration (TFH) method (I), thin film hydration followed by freeze–thaw cycles (II), and direct injection method (III). Reprinted with permission from ref. 115 (b) fluorescent microscopy images of lung tissue with fluorescently labeled HH reagent in both healthy (I) and bleomycin-challenged (II) lung tissue, displaying deposition locations of HH reagent via intranasal treatment. Images on right are high magnification of the squared regions. Reprinted with permission from ref. 116 (c) schematic of anti-TB drug-loaded PVA–chitosan–TPP hydrogel matrix. Reprinted with permission from ref. 117.



end-stage IPF, lung transplantation is often the treatment choice. Therefore, there is a pressing need for novel anti-fibrotic therapies that can effectively slow down disease progression and improve clinical outcomes. Interleukin-10 (IL-10) is a cytokine with powerful anti-inflammatory and anti-fibrosis properties, which makes it an attractive treatment candidate for IPF. The ideal would involve the direct and sustained release of IL-10 into lung tissue, utilizing a carrier with excellent biocompatibility and minimal toxicity to lung tissue. Therefore, Vinicio *et al.* developed HH-10, a hydrogel produced by the chemical cross-linking of hyaluronic acid and heparin, which aims to retain water (hyaluronic acid) and combine with IL-10 (heparin) (Fig. 13b). The HH-10 formulation represents an effective method to deliver the therapeutic dose of IL-10 directly to the lungs through inhalation, and can be used alone or in combination with existing treatment methods, thereby preserving lung function and improving prognosis of IPF patient. Most importantly, the formulation may be widely used in other lung diseases characterized by excessive fiber hyperplasia (such as scleroderma and radiation-induced fibrosis).<sup>116</sup>

Tuberculosis is an infectious disease caused by *Mycobacterium tuberculosis* and the standard treatment involves a combination of oral medications such as isoniazid, rifampicin, ethambutol and pyrazinamide. However, these medications can cause discomfort and liver damage in patients, and the emergence of drug-resistant bacteria is a significant concern. Developing an extended drug release system that allows for slow and targeted drug release at the site of infection could offer several advantages in tuberculosis treatment, including reduced drug dosage, minimized liver side effects, and decreased frequency of drug administration. K. Mulia *et al.* prepared polyvinyl alcohol-chitosan-tripolyphosphate hydrogel by solvent casting-evaporation method as a sustained-release preparation of anti-tuberculosis drugs (Fig. 13c). The results of X-ray diffraction and scanning electron microscope showed that chitosan reduced the crystallinity of polyvinyl alcohol (PVA) hydrogel, and the polymer formed a homogeneous mixture.

The addition of chitosan reduced the encapsulation efficiency and drug release rate. In phosphate buffer solution with pH 7.4, the formulation of 80% PVA-20% chitosan hydrogel has the highest drug release rate in a short time. In the matrix preparation containing only PVA, the drug loading efficiency is the highest, while the addition of sodium tripolyphosphate improves the drug loading efficiency and reduces the drug release. The hydrogel matrix formula of PVA-chitosan tripolyphosphate exhibited potential as an extended delivery system for anti-tuberculosis drugs.<sup>117</sup>

## 5. Conclusion and perspectives

The integration of medicine and materials science has led to significant advancements in the field of gel materials for medical applications. Researchers have increasingly recognized the potential of gel materials in addressing clinical challenges related to respiratory diseases. Gel materials will play an important role in the diagnosis and treatment of respiratory diseases in the future (Fig. 14). This article reviews the diverse roles of gel materials in the diagnosis and treatment of respiratory diseases, including their use in radiotherapy for lung cancer, drug delivery system and managing complications following thoracoscopic pneumonectomy. In addition to the application in the diagnosis and treatment of malignant lung diseases, gel materials can also be used in benign lung diseases, such as the improvement of drug delivery methods for pulmonary infectious diseases, preoperative localization of pulmonary nodules and embolization treatment of pulmonary vascular diseases. Despite the progress made in the laboratory simulation stage, the translation of gel materials into practical clinical applications is still a challenge. Safety considerations regarding the use of gel materials in living organisms remain a crucial aspect that requires further investigation. Researchers are actively working on addressing these concerns and expediting the

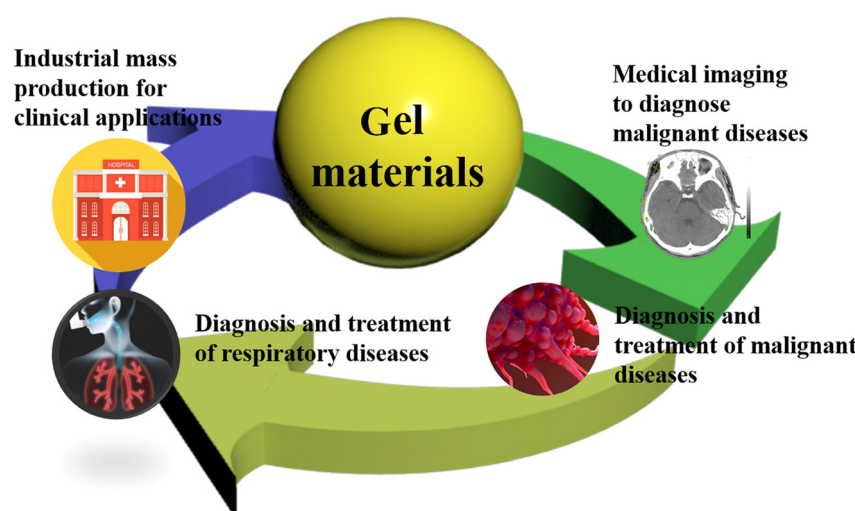


Fig. 14 Future development of gel materials for diagnosis and treatment of respiratory diseases.



market availability of gel materials for the benefit of humanity. Furthermore, it is worth noting the importance of imaging techniques in the diagnosis of respiratory diseases. Surprisingly, there is currently no reported application of gel materials as contrast agents in the diagnosis of respiratory conditions. This highlights a potential new research direction to explore the use of gel materials in imaging modalities for respiratory diseases. In conclusion, the current clinical application of gel-based nanocomposites in respiratory diseases primarily focuses on drug delivery systems. To address the limitations of nanogels, it is important to pursue simple yet efficient designs with low toxicity. Developing nanogels with prolonged release cycles and well-controlled release profiles can enhance therapeutic efficacy while minimizing toxicity. Furthermore, further research is needed to explore the safety, functional modification, mechanical properties and biocompatibility of gels. This will help to optimize the properties of gel materials and improve their performance in medical applications. Looking ahead, the future goal is to develop intelligent nano-gel carriers that integrate diagnosis and treatment functionalities. These carriers should exhibit high drug-loading capacity, site-specific responsiveness for imaging and drug release, and maximize the potential of gel-based nanocomposites in the medical field. This advancement would provide new strategies for the diagnosis and treatment of respiratory diseases.

## Data availability

No data was used for the research described in the article.

## Conflicts of interest

The authors declare that they do not possess any known conflicting financial interests or personal relationships that could have influenced the work reported in this manuscript.

## Acknowledgements

This work received financial support from the Clinical Research and Cultivation Plan Project of the Second Affiliated Hospital of Anhui Medical University (2021LCZD09), the Translational Medicine Research Fund Project of the Second Affiliated Hospital of Anhui Medical University (2022ZHYJ07), Starting Fund for Scientific Research of High-Level Talents, Anhui Agricultural University (rc382108), the Key Research and Development Plan of Anhui Province (2022e07020037), Health Research Project of Anhui Province (AHWJ2022b014) and the Anhui Province Natural Science Foundation (2208085MH194), Entrepreneurship Training Plan Project of Anhui Province (X202210364291), Shen-Nong Scholar Program of Anhui Agricultural University (rc382101) and National College Student Innovation and Entrepreneurship Training Plan Project (S202210364094).

## References

- 1 N. Khaltaev and S. Axelrod, *J. Thorac. Dis.*, 2019, **11**, 2643–2655.
- 2 H. J. Xiang and Y. Chen, *View*, 2020, 20200016.
- 3 A. Keller, *Faraday Discuss.*, 1995, **101**, 1–49.
- 4 M. A. Qureshi and F. Khatoon, *J. Sci.: Adv. Mater. Devices*, 2019, **4**, 201–212.
- 5 I. Neamtu, A. G. Rusu, A. Diaconu, L. E. Nita and A. P. Chiriac, *Drug Delivery*, 2017, **24**, 539–557.
- 6 L. L. Hu, C. L. Song, H. Y. Li, Y. Gao, J. Zhang, T. Gao, Y. H. Wei, Z. R. Xu, W. M. Xue, S. P. Huang, H. Y. Wen, Z. G. Li and J. Wu, *Macromol. Biosci.*, 2023, 2200565.
- 7 H. L. Guo, S. Huang, X. F. Yang, J. P. Wu, T. B. Kirk, J. K. Xu, A. D. Xu and W. Xue, *ACS Appl. Mater. Interfaces*, 2021, **13**, 61638–61652.
- 8 B. Cai, Q. Zou, Y. Zuo, Q. J. Mei, J. Q. Ma, L. L. Lin, L. Chen and Y. B. Li, *ACS Appl. Mater. Interfaces*, 2018, **10**, 25099–25112.
- 9 R. C. op 't Veld, O. I. van den Boomen, D. M. S. Lundvig, E. M. Bronkhorst, P. H. J. Kouwer, J. A. Jansen, E. Middelkoop, J. W. Von den Hoff, A. E. Rowan and F. Wagener, *Biomaterials*, 2018, **181**, 392–401.
- 10 P. F. Sun, T. Huang, X. X. Wang, G. N. Wang, Z. J. Liu, G. S. Chen and Q. L. Fan, *Biomacromolecules*, 2020, **21**, 556–565.
- 11 Y. F. Fang, G. Z. Li, C. L. Huang, K. Q. Huang, Y. Zhao, T. Q. Nie and J. Wu, *Int. J. Biol. Macromol.*, 2023, **229**, 123–135.
- 12 B. Pruitt, *Nursing*, 2021, **51**, 22–29.
- 13 J. Sauleda, B. Nunez, E. Sala and J. B. Soriano, *Med. Sci.*, 2018, **6**, 110.
- 14 G. Raghu, H. R. Collard, J. J. Egan, F. J. Martinez, J. Behr, K. K. Brown, T. V. Colby, J. F. Cordier, K. R. Flaherty, J. A. Lasky, D. A. Lynch, J. H. Ryu, J. J. Swigris, A. U. Wells, J. Ancochea, D. Bouros, C. Carvalho, U. Costabel, M. Ebina, D. M. Hansell, T. Johkoh, D. S. Kim, T. E. King, Y. Kondoh, J. Myers, N. L. Muller, A. G. Nicholson, L. Richeldi, M. Selman, R. F. Dudden, B. S. Griss, S. L. Protzko, H. J. Schunemann and A. E. J. A. Comm, *Am. J. Respir. Crit. Care Med.*, 2011, **183**, 788–824.
- 15 Y. Nakamura and T. Suda, *Clin. Med. Insights: Circ., Respir. Pulm. Med.*, 2015, **9**, 163–171.
- 16 Y. Zaizen and J. Fukuoka, *Surg. Pathol. Clin.*, 2020, **13**, 91–118.
- 17 D. Y. Feng, Y. Q. Zhou, Y. F. Xing, C. F. Li, Q. Lv, J. Dong, J. Qin, Y. F. Guo, N. Jiang, C. C. Huang, H. T. Hu, X. H. Guo, J. Chen, L. H. Yin, T. T. Zhang and X. Li, *Ther. Clin. Risk Manage.*, 2018, **14**, 1975–1986.
- 18 A. Jakubczyc and C. Neurohr, *Dtsch. Med. Wochenschr.*, 2020, **145**, 470–473.
- 19 A. Aslam, I. Anwar and A. Tariq, *J. Pak. Med. Assoc.*, 2021, **71**, 446–448.
- 20 R. M. Chalmers, R. S. Howard, C. M. Wiles and G. T. Spencer, *Q. J. Med.*, 1994, **87**, 423–429.
- 21 Z. Gyurcsik, N. Bodnar, Z. Szekanecz and S. Szanto, *Zeitschrift Fur Rheumatologie*, 2013, **72**, 997–1004.



22 O. Rogoveanu, D. Kamal, C. T. Streba and R. Traistaru, *Curr. Health Sci. J.*, 2015, **41**, 406–414.

23 A. Torii, Y. Ono, S. Obayashi, A. Kitahara, K. Oshinden, Y. Horio, K. Niimi, N. Hayama, T. Oguma, K. Hatanaka, K. Asano and Y. Ito, *Int. Med.*, 2022, **61**, 2649–2653.

24 C. H. J. Won and M. Kryger, *Clin. Chest Med.*, 2014, **35**, 505–512.

25 J. P. Laaban, *La Revue du praticien*, 1993, **43**, 1911–1917.

26 C. F. Vogelmeier, G. J. Criner, F. J. Martinez, A. Anzueto, P. J. Barnes, J. Bourbeau, B. R. Celli, R. C. Chen, M. Decramer, L. M. Fabbri, P. Frith, D. M. G. Halpin, M. V. L. Varela, M. Nishimura, N. Roche, R. Rodriguez-Roisin, D. D. Sin, D. Singh, R. Stockley, J. Vestbo, J. A. Wedzicha and A. Agusti, *Am. J. Respir. Crit. Care Med.*, 2017, **195**, 557–582.

27 C. Raherison and P. O. Girodet, *Eur. Res. Rev.*, 2009, **18**, 213–221.

28 J. Park, H.-J. Kim, C.-H. Lee, C. H. Lee and H. W. Lee, *Environ. Res.*, 2021, **194**, 110703.

29 R. X. Zhu, X. H. Nie, Y. H. Chen, J. Chen, S. W. Wu and L. H. Zhao, *Am. J. Med. Sci.*, 2020, **359**, 354–364.

30 C. Peng, Y. J. Yan, Z. Li, Y. X. Jiang and Y. Cai, *Medicine*, 2020, **99**, e21908.

31 K. Bartziokas, A. Papaporfyriou, G. Hillas, A. I. Papaioannou and S. Loukides, *Postgrad. Med.*, 2023, **135**, 327–333.

32 E. National Asthma and P. Prevention, *J. Allergy Clin. Immunol.*, 2007, **120**, S94–138.

33 Y. H. Hsiao, Y. J. Lin, T. H. Jeng, K. C. Su, H. K. Ko, S. N. Yang, D. W. Perng and Y. R. Kou, *J. Chin. Med. Assoc.*, 2022, **85**, 859–865.

34 H. K. Reddel, L. B. Bacharier, E. D. Bateman, C. E. Brightling, G. G. Brusselle, R. Buhl, A. A. Cruz, L. Duijts, J. M. Drazen, J. M. FitzGerald, L. J. Fleming, H. Inoue, F. W. Ko, J. A. Krishnan, M. L. Levy, J. T. Lin, K. Mortimer, P. M. Pitrez, A. Sheikh, A. A. Yorgancioglu and L. P. Boulet, *Am. J. Respir. Crit. Care Med.*, 2022, **205**, 17–35.

35 J. L. Lin, J. F. Xu and J. M. Qu, *Ann. Am. Thorac. Soc.*, 2016, **13**, 609–616.

36 P. A. Flume, J. D. Chalmers and K. N. Olivier, *Lancet*, 2018, **392**, 880–890.

37 A. E. O'Donnell, *N. Engl. J. Med.*, 2022, **387**, 533–545.

38 A. F. Barker, A. Bergeron, W. N. Rom and M. I. Hertz, *N. Engl. J. Med.*, 2014, **370**, 1820–1828.

39 A. J. Colom and A. M. Teper, *Pediatric Pulmonology*, 2009, **44**, 1065–1069.

40 B. Afessa, M. R. Litzow and A. Tefferi, *Bone Marrow Transplant.*, 2001, **28**, 425–434.

41 M. I. Hertz, D. O. Taylor, E. P. Trulock, M. M. Boucek, P. J. Mohacs, L. B. Edwards and B. M. Keck, *J. Heart Lung Trans.*, 2002, **21**, 950–970.

42 T. E. King, *Semin. Res. Critical Care Med.*, 2003, **24**, 567–576.

43 L. J. Rubin, *Chest*, 1993, **104**, 236–250.

44 A. M. Wendelboe and G. E. Raskob, *Circ. Res.*, 2016, **118**, 1340–1347.

45 A. Boucly, B. Girerd, D. Bourlier, S. Nemlaghi, J. Caliez, L. Savale, X. Jais, P. Dorfmuller, G. Simonneau, O. Sitbon, M. Humbert and D. Montani, *Rev. Mal. Respir.*, 2018, **35**, 160–170.

46 C. R. Miller, *Pediatr. Radiol.*, 2012, **42**, 647–652.

47 A. Huertas, B. Girerd, P. Dorfmuller, D. O'Callaghan, M. Humbert and D. Montani, *Expert Rev. Respir. Med.*, 2011, **5**, 217–231.

48 A. Dhala, *Clin. Dev. Immunol.*, 2012, **2012**, 854941.

49 C. C. Tsang, J. L. L. Teng, S. K. P. Lau and P. C. Y. Woo, *J. Fungi*, 2021, **7**, 636.

50 W. Cruz-Knight and L. Blake-Gumbs, *Primary Care*, 2013, **40**, 743–756.

51 P. Prombutara, T. A. P. Siregar, T. Laopanupong, P. Kanjanasirirat, T. Khumpanied, S. Borwornpinyo, A. Rai, A. Chaiprasert, P. Palittapongarnpim and M. Ponpuak, *Virulence*, 2022, **13**, 1810–1826.

52 E. A. Borodulina, V. V. Piskun, M. V. Uraksina and A. T. Shubina, *Klinicheskaiia laboratornaia diagnostika*, 2022, **67**, 544–549.

53 K. Dheda, T. Gumbo, G. Maartens, K. E. Dooley, R. McNerney, M. Murray, J. Furin, E. A. Nardell, L. London, E. Lessem, G. Theron, P. van Helden, S. Niemann, M. Merker, D. Dowdy, A. Van Rie, G. K. H. Siu, J. G. Pasipanodya, C. Rodrigues, T. G. Clark, F. A. Sirgel, A. Esmail, H. H. Lin, S. R. Atre, H. S. Schaaf, K. C. Chang, C. Lange, P. Nahid, Z. F. Udwadia, C. R. Horsburgh, G. J. Churchyard, D. Menzies, A. C. Hesselung, E. Nuermberger, H. McIlleron, K. P. Fennelly, E. Goemaere, E. Jaramillo, M. Low, C. M. Jara, N. Padayatchi and R. M. Warren, *Lancet Respir. Med.*, 2017, **5**, 291–360.

54 R. L. Siegel, K. D. Miller, H. E. Fuchs and A. Jemal, *Ca-Cancer J. Clin.*, 2022, **72**, 7–33.

55 L. M. O'Keeffe, G. Taylor, R. R. Huxley, P. Mitchell, M. Woodward and S. A. E. Peters, *Bmj Open*, 2018, **8**, e021611.

56 S. van der Bij, H. Koffijberg, V. Lenters, L. Portengen, K. G. M. Moons, D. Heederik and R. C. H. Vermeulen, *Cancer, Causes Control*, 2013, **24**, 1–12.

57 L. Zhu, Y. Shu, C. Liu, Y. W. Zhu, Y. Xiao, J. Ran and C. X. Zhang, *Nutrition*, 2022, **99–100**, 111676.

58 J. Rodriguez-Canales, E. Parra-Cuentas and I. I. Wistuba, *Cancer Treat. Res.*, 2016, **170**, 25–46.

59 S. H. Gao, G. B. Zhang, Y. F. Lian, L. Yan and H. X. Gao, *Cell. Mol. Biol.*, 2020, **66**, 93–97.

60 F. Tas, E. Bilgin, D. Tastekin, K. Erturk and D. Duranyildiz, *Biomed. Rep.*, 2016, **4**, 485–488.

61 E. T. Korkmaz, D. Koksal, F. Aksu, Z. G. Dikmen, D. Icen, E. Maden, S. Onder, F. Akbıyık and S. Emri, *Clin. Biochem.*, 2018, **58**, 15–19.

62 R. Molina, J. M. Auge, X. Bosch, J. M. Escudero, N. Vinolas, R. Marrades, J. Ramirez, E. Carcereny and X. Filella, *Tumor Biol.*, 2009, **30**, 121–129.

63 K. Pisters, M. G. Kris, L. E. Gaspar, N. Ismaila and A. Adjuvant Systemic Therapy, *J. Clin. Oncol.*, 2022, **40**, 1127–1129.



64 S. Haefner, M. Rohn, P. Frank, G. Paschew, M. Elstner and A. Richter, *Gels*, 2016, **2**, 10.

65 S. Mallakpour and A. Jarahiyan, *Ultrason. Sonochem.*, 2017, **37**, 128–135.

66 N. M. Hosny, M. Abbass, F. Ismail and H. M. N. El-Din, *Polym. Bull.*, 2023, **80**, 4573–4588.

67 E. Marsano, S. Gagliardi, F. Ghioni and E. Bianchi, *Polymer*, 2000, **41**, 7691–7698.

68 J. Wu, Z. M. Wu, X. J. Sun, S. C. Yuan, R. L. Zhang, Q. L. Lu and Y. Q. Yu, *J. Chin. Chem. Soc.*, 2017, **64**, 231–238.

69 X. F. Wang, L. Zhang and M. H. Liu, *Acta Phys.-Chim. Sin.*, 2016, **32**, 227–238.

70 X. Z. Yan, D. H. Xu, X. D. Chi, J. Z. Chen, S. Y. Dong, X. Ding, Y. H. Yu and F. H. Huang, *Adv. Mater.*, 2012, **24**, 362–369.

71 X. Z. Yan, D. H. Xu, J. Z. Chen, M. M. Zhang, B. J. Hu, Y. H. Yu and F. H. Huang, *Polym. Chem.*, 2013, **4**, 3312–3322.

72 Y. M. Zhu, Z. C. Yao, Y. S. Liu, W. Zhang, L. L. Geng and T. Ni, *Int. J. Nanomed.*, 2020, **15**, 333–346.

73 Z. Zhu, Y. Yang, Y. Guan, J. H. Xue and L. L. Cui, *J. Mater. Chem. A*, 2016, **4**, 15536–15545.

74 Y. Zhuang, Y. Kong, X. C. Wang and B. Y. Shi, *New J. Chem.*, 2019, **43**, 7202–7208.

75 H. Nabipour, S. B. Nie, X. Wang, L. Song and Y. Hu, *Cellulose*, 2020, **27**, 2237–2251.

76 L. J. Huang, M. He, B. B. Chen and B. Hu, *J. Mater. Chem. A*, 2016, **4**, 5159–5166.

77 M. Hagiwara, *Anal. Biochem.*, 2022, **652**, 114751.

78 C. Sakuma, Y. Tomioka, C. Li, T. Shibata, M. Nakagawa, Y. Kurosawa, T. Arakawa and T. Akuta, *Int. J. Biol. Macromol.*, 2021, **172**, 589–596.

79 C. Sakuma, M. Nakagawa, Y. Tomioka, T. Maruyama, K. Entzminger, J. K. Fleming, T. Shibata, Y. Kurosawa, C. J. Okumura, T. Arakawa and T. Akuta, *Biotechniques*, 2022, **72**, 207–218.

80 J. M. Zaetta, M. O. Licht, J. S. Fisher, R. L. Avelar and G. Bio-Seal Study, *J. Vascular Int. Radiol.*, 2010, **21**, 1235–1243.

81 F. Longo, R. F. Grasso, G. Tacchi, L. Frasca, E. Faiella and P. Crucitti, *Med. Sci.*, 2022, **10**, 54.

82 Y. J. Liu, A. Ibricevic, J. A. Cohen, J. L. Cohen, S. P. Gunsten, J. M. J. Frechet, M. J. Walter, M. J. Welch and S. L. Brody, *Mol. Pharmaceutics*, 2009, **6**, 1891–1902.

83 M. O. Maiwand and G. Asimakopoulos, *Technol. Cancer Res. Treat.*, 2004, **3**, 143–150.

84 A. A. Gage and J. Baust, *Cryobiology*, 1998, **37**, 171–186.

85 M. L. Etheridge, J. Choi, S. Ramadhyani and J. C. Bischof, *J. Biomech. Eng.*, 2013, **135**, 021002.

86 S. A. Agnes and J. Anitha, *J. Med. Imaging*, 2022, **9**, 052402.

87 M. P. Rivera, A. C. Mehta and M. M. Wahidi, *Chest*, 2013, **143**, E142–E165.

88 S. Nakashima, A. Watanabe, T. Obama, G. Yamada, H. Takahashi and T. Higami, *Ann. Thorac. Surg.*, 2010, **89**, 212–218.

89 T. Iguchi, T. Hiraki, H. Gobara, H. Fujiwara, Y. Matsui, S. Miyoshi and S. Kanazawa, *Eur. Radiol.*, 2016, **26**, 114–121.

90 A. Chella, M. Lucchi, M. C. Ambrogi, G. Menconi, F. M. A. Melfi, A. Gonfiotti, G. Boni and C. A. Angeletti, *Eur. J. Cardiol.*, 2000, **18**, 17–21.

91 A. Mogi, T. Yajima, K. Tomizawa, R. Onozato, S. Tanaka and H. Kuwano, *Ann. Thorac. Cardiovasc. Surg.*, 2015, **21**, 435–439.

92 R. Yoshida, T. Yoshizako, S. Tanaka, S. Ando, M. Nakamura, K. Kishimoto and H. Kitagaki, *Clin. Imaging*, 2021, **74**, 84–88.

93 H. Y. Seol, H. Y. Ahn, H. S. Chung and J. S. Eom, *General Thorac. Cardiovasc. Surg.*, 2020, **68**, 87–90.

94 A. K. Saxena, *J. Thorac. Cardiovasc. Surg.*, 2010, **139**, 496–497.

95 S. Qiu, N. J. Ge, D. K. Sun, S. Zhao, J. F. Sun, Z. B. Guo, K. Hu and N. Gu, *IEEE Trans. Biomed. Eng.*, 2016, **63**, 730–736.

96 J. Malicki, *Rep. Practical Oncol. Radiotherapy*, 2012, **17**, 63–65.

97 J. C. Gore, Y. S. Kang and R. J. Schulz, *Phys. Med. Biol.*, 1984, **29**, 1189–1197.

98 M. Jaszczałk, R. Wach, P. Maras, M. Dudek and M. Kozicki, *Phys. Med. Biol.*, 2018, **63**, 175010.

99 N. Gharehaghaji and H. A. Dadgar, *J. Cancer Res. Ther.*, 2018, **14**, 278–286.

100 M. Kozicki, K. Kwiatos, M. Dudek and Z. Stempien, *J. Photochem. Photobiol. A*, 2018, **351**, 197–207.

101 M. Kozicki, K. Kwiatos, S. Kadlubowski and M. Dudek, *Phys. Med. Biol.*, 2017, **62**, 5668–5690.

102 M. Kozicki, M. Jaszczałk, P. Maras, R. Nagliki, M. Dudek, S. Kadlubowski and R. Wach, *Radiat. Phys. Chem.*, 2021, **185**, 109479.

103 P. Lee, C. N. Lok, C. M. Che and W. J. Kao, *Pharm. Res.*, 2019, **36**, 61.

104 L. Hosta-Rigau, R. Chandrawati, E. Saveriades, P. D. Odermatt, A. Postma, F. Ercole, K. Breheney, K. L. Wark, B. Stadler and F. Caruso, *Biomacromolecules*, 2010, **11**, 3548–3555.

105 J. W. Li, D. D. Yuan, X. J. Zheng, X. Y. Zhang, X. M. Li and S. S. Zhang, *Sci. China: Chem.*, 2020, **63**, 546–553.

106 Y. Gao, F. Z. Ren, B. Y. Ding, N. Y. Sun, X. Liu, X. Y. Ding and S. Gao, *J. Drug Targeting*, 2011, **19**, 516–527.

107 S. Heine, A. Aguilar-Pimentel, D. Russkamp, F. Alessandrini, V. Gailus-Durner, H. Fuchs, M. Ollert, R. Bredehorst, C. Ohnmacht, U. M. Zissler, M. H. de Angelis, C. B. Schmidt-Weber and S. Blank, *Pharmaceutics*, 2022, **14**, 1527.

108 T. L. Bowersock, W. S. W. Shalaby, M. Levy, M. L. Samuels, R. Lallone, M. R. White, D. L. Borie, J. Lehmyer and K. Park, *Am. J. Vet. Res.*, 1994, **55**, 502–509.

109 A. Tremblay, S. Dumitriu, D. R. Stather, P. MacEachern, O. Illanes and M. M. Kelly, *Exp. Lung Res.*, 2012, **38**, 475–482.

110 C. Chittasupho, J. Angklomklew, T. Thongnopkoon, W. Senavongse, P. Jantrawut and W. Rukksiriwanich, *Polymers*, 2021, **13**, 3580.

111 X. H. Zhou, X. L. He, K. Shi, L. P. Yuan, Y. Yang, Q. Y. Liu, Y. Ming, C. Yi and Z. Y. Qian, *Adv. Sci.*, 2020, **7**, 202001442.



112 J. Xu, C. X. Zhang, C. Cheng, J. Yang, C. X. Li, X. Liu and Y. Sang, *J. Appl. Biomater. Biomech.*, 2022, **20**, 22808000211073729.

113 J. Du, I. M. El-Sherbiny and H. D. Smyth, *AAPS PharmSciTech*, 2014, **15**, 1535–1544.

114 H. Y. Hsieh, W. Y. Lin, A. L. Lee, Y. C. Li, Y. J. Chen, K. C. Chen and T. H. Young, *PLoS One*, 2020, **15**, e0227784.

115 A. Jose, P. K. Mandapalli and V. V. K. Venuganti, *J. Liposome Res.*, 2016, **26**, 139–147.

116 E. A. Shamskhou, M. J. Kratochvil, M. E. Orcholski, N. Nagy, G. Kaber, E. Steen, S. Balaji, K. Yuan, S. Keswani, B. Danielson, M. Gao, C. Medina, A. Nathan, A. Chakraborty, P. L. Bollyky and V. A. D. Perez, *Biomaterials*, 2019, **203**, 52–62.

117 K. Mulia, S. A. Chadarwati, A. J. Rahyussalim and E. A. Krisanti, *IOP Conf. Ser., Mater. Sci. Eng.*, 2019, **703**, 012010.

